

ABSTRACT

A system transient model for the Browns Ferry Nuclear Plant based on the RETRAN program is described. The model is applicable to a wide range of transients but is primarily intended for analysis of the limiting pressurization transients considered for reload core licensing. The model is qualified by comparisons to a range of startup test transients and to special turbine trip transients performed on a boiling water reactor of essentially identical design as the Browns Ferry units. The results of a special NRC test problem with comparisons to other codes' calculations are also presented.

A representative application of the model for licensing basis calculations of the limiting pressurization transients (based on Browns Ferry unit 3 at projected end of cycle 5 conditions) is presented. Results of extensive sensitivity studies are presented for the licensing basis calculations. Two procedures for determining conservative critical power ratio limits from the model results are developed and their use in updating plant technical specifications demonstrated.

**REGULATORY DOCKET FILE COPY**

8207300243 820723  
PDR ADOCK 05000259  
P PDR



## ACKNOWLEDGEMENT

The authors wish to acknowledge the assistance provided by many other individuals in several TVA organizations during the course of development of this model. The assistance of J. Naser and L. Agee of EPRI and J. McFadden of Energy Incorporated is also gratefully acknowledged. Special thanks are due to Vivian Davis for her diligent efforts in typing the manuscript. The assistance of John Strange in performing some of the analyses in chapter 7 and Sheree Hutcherson in preparing many of the figures is also appreciated.



## TABLE OF CONTENTS

	<u>PAGE</u>
ABSTRACT . . . . .	1
ACKNOWLEDGEMENT. . . . .	11
1. INTRODUCTION. . . . .	1
1.1 Purpose . . . . .	1
1.2 Applicable Events . . . . .	1
1.3 The RETRAN Code . . . . .	3
1.4 Thermal Limits Evaluation . . . . .	4
1.5 The BFNP Model. . . . .	4
2. DESCRIPTION OF MODEL. . . . .	6
2.1 Introduction. . . . .	6
2.2 Model Geometry. . . . .	11
2.2.1 Recirculation Loops. . . . .	11
2.2.2 Feedwater and Steam Lines. . . . .	17
2.2.3 Vessel Internals . . . . .	18
2.2.4 Core Region. . . . .	19
2.3 System Components . . . . .	20
2.3.1 Recirculation Pumps. . . . .	25
2.3.2 Jet Pumps. . . . .	25
2.3.3 Steam Separators . . . . .	28
2.3.4 Safety/Relief Valves . . . . .	29
2.3.5 Core Hydraulics. . . . .	31
2.4 Trips and Control Models. . . . .	32
2.4.1 Trips. . . . .	32
2.4.2 Controls . . . . .	36
2.4.2.1 Sensed Inputs and Miscellaneous Calculations. . . . .	36
2.4.2.2 Reactor Water Level Modeling. . . . .	42
2.4.2.3 Feedwater Control System. . . . .	49
2.4.2.4 Electro-Hydraulic Control System. . . . .	51
2.4.2.5 Recirculation Control System. . . . .	57

TABLE OF CONTENTS (Continued)

	<u>PAGE</u>
2.5 Condition Specific Inputs . . . . .	63
2.5.1 One-Dimensional Kinetics Data. . . . .	63
2.5.1.1 Procedure for Generating Kinetics Data. . . . .	64
2.5.1.2 Verification of Procedures for Generating Kinetics Data . . . . .	68
2.5.1.3 Generic Kinetics Inputs . . . . .	72
2.5.2 Initialization . . . . .	77
3. COMPARISONS TO BFNP STARTUP TESTS . . . . .	82
3.1 Feedwater Transients. . . . .	83
3.1.1 Level Change . . . . .	83
3.1.2 Feedwater Turbine Trip . . . . .	86
3.2 Recirculation System Transients . . . . .	93
3.2.1 Two-Loop Trips . . . . .	97
3.2.2 One M-G Trip . . . . .	110
3.3 Pressurization Transient. . . . .	119
3.3.1 Sequence of Events . . . . .	126
3.3.2 Model Comparisons to Measurements. . . . .	127
4. COMPARISONS TO PEACH BOTTOM TURBINE TRIP TESTS. . . . .	137
4.1 Peach Bottom Turbine Trip Tests . . . . .	137
4.1.1 Test Objectives. . . . .	137
4.1.2 Test Description . . . . .	138
4.1.3 Reactor Description. . . . .	139
4.2 RETRAN Peach Bottom Model . . . . .	140
4.2.1 Description. . . . .	140
4.2.2 Modifications to BFNP Model. . . . .	142
4.2.3 Initial Conditions . . . . .	142
4.2.4 Model Inputs . . . . .	145
4.3 RETRAN Analyses of Peach Bottom Tests . . . . .	147
4.3.1 RETRAN Calculations. . . . .	147
4.3.2 Measured Data. . . . .	148
4.3.3 Data Comparisons . . . . .	151

TABLE OF CONTENTS (Continued)

	<u>PAGE</u>
4.3.3.1 Pressure and Flow Comparisons . . . . .	151
4.3.3.2 Power and Reactivity Comparisons. . . . .	167
4.4 CPR Calculations. . . . .	191
4.4.1 Calculations . . . . .	191
4.4.2 Measured (Inferred) Delta-CPR. . . . .	192
4.4.3 Delta-CPR Comparisons. . . . .	193
5. NRC TEST PROBLEM. . . . .	196
5.1 Description of Test Problem . . . . .	196
5.2 Model Inputs. . . . .	197
5.3 Results for Test Problem. . . . .	199
6. REPRESENTATIVE LICENSING BASIS ANALYSES . . . . .	217
6.1 Licensing Basis Inputs. . . . .	217
6.1.1 Core Exposure. . . . .	217
6.1.2 Initial State Point. . . . .	219
6.1.3 Scram Reactivity . . . . .	220
6.1.4 Fuel Rod Gap Conductance . . . . .	222
6.1.5 Separator Inertia. . . . .	222
6.1.6 Equipment Specifications . . . . .	223
6.1.7 Hot Channel Modeling . . . . .	223
6.2 Generator Load Rejection Without Bypass . . . . .	225
6.2.1 Sequence of Events . . . . .	225
6.2.2 Results of RETRAN Analysis . . . . .	226
6.3 Feedwater Controller Failure. . . . .	238
6.3.1 Sequence of Events . . . . .	239
6.3.2 Results of RETRAN Analysis . . . . .	240
6.4 Main Steam Isolation Valve Closure with Flux Scram. . . . .	247
6.4.1 Sequence of Events . . . . .	252
6.4.2 Results of RETRAN Analysis . . . . .	253

TABLE OF CONTENTS (Continued)

	<u>PAGE</u>
6.5 Summary of Transient Results. . . . .	261
7. MODEL SENSITIVITY STUDIES . . . . .	267
7.1 GLRWOB Sensitivity Studies. . . . .	268
7.1.1 Nuclear Model. . . . .	268
7.1.1.1 Void Reactivity . . . . .	268
7.1.1.2 Scram Reactivity. . . . .	273
7.1.1.3 Doppler Reactivity. . . . .	273
7.1.1.4 Prompt Moderator Heating. . . . .	274
7.1.2 Core Thermal-Hydraulic Modeling. . . . .	274
7.1.2.1 Fuel Pin Modeling . . . . .	275
7.1.2.2 Core Pressure Drop. . . . .	276
7.1.2.3 Core and Core Bypass Modeling . . . . .	276
7.1.2.4 Void Models . . . . .	278
7.1.3 Recirculation System Model . . . . .	279
7.1.3.1 Recirculation Loop. . . . .	280
7.1.3.2 Jet Pump Model. . . . .	280
7.1.3.3 Steam Separator Model . . . . .	281
7.1.4 Vessel and Steam Line Nodes. . . . .	282
7.1.4.1 Vessel Nodes. . . . .	282
7.1.4.2 Steam Line Model. . . . .	283
7.1.5 Miscellaneous Sensitivity Results. . . . .	285
7.2 FWCF Sensitivity Studies. . . . .	286
7.2.1 Nuclear Model. . . . .	286
7.2.2 Core Thermal-Hydraulics Modeling . . . . .	286
7.2.3 Recirculation System Model . . . . .	288
7.2.4 Steam Line Modeling. . . . .	288
7.2.5 Miscellaneous. . . . .	289
7.3 MSIVC Sensitivity Studies . . . . .	290

TABLE OF CONTENTS (Continued)

	<u>PAGE</u>
8. ALLOWANCES FOR MODEL UNCERTAINTIES. . . . .	294
8.1 Option A Operating Limit MCPR . . . . .	294
8.2 Option B Operating Limit MCPR . . . . .	296
8.2.1 Statistical Process for Margin Evaluation. . . . .	296
8.2.2 Model Response Surface . . . . .	297
8.2.3 Statistical Adjustment Factors . . . . .	303
8.3 Determination of Actual Operating Limit MCPR. . . . .	305



## 6. REPRESENTATIVE LICENSING BASIS ANALYSES

The three limiting pressurization transients for reload licensing analyses were identified in chapter 1 as: the generator load rejection with failure of the turbine bypass system (GLRWOB), feedwater controller failure to maximum demand (FWCF), and closure of all main steam isolation valves with indirect scram on high neutron flux (MSIVC). The basis for selecting these three events as limiting was given in chapter 1 and discussed in reference 6-1.

This chapter will describe the model inputs and initial conditions for licensing basis analyses and indicate how these inputs compare to expected values. Representative results for each of the three events will be shown using a hypothetical licensing basis analysis for Browns Ferry unit 3 at conditions projected for the end of its fifth operating cycle.

### 6.1 Licensing Basis Inputs

The basic model utilized for licensing analyses was described in chapter 2. There are some conservative inputs for the licensing basis analyses and conservative initial conditions are employed. Table 6-1 shows the relationship of licensing basis model inputs and initial conditions to the expected values. The "expected" values and conditions are meant only to show potential conservatisms in the licensing basis modeling and not to define a practical "best estimate" model.

#### 6.1.1 Core Exposure

The licensing analyses are performed at the maximum cycle exposure in the interval for which the analysis applies (e.g., BOC to EOC-2 GWD/MT, BOC

Table 6-1

## Transient Model Inputs &amp; Initial Conditions Compared to Expected Values

<u>Item</u>	<u>Expected Value</u>	<u>Licensing Basis Analysis</u>
Cycle Exposure	Inside interval	Max. value for interval being analyzed
Power/Exposure Distribution	Nominal	Conservative target
Initial Power (%NBR)	$\leq 100.$	104.5
Initial Steam Flow (%NBR)	$\leq 100.$	105.0
Initial Core Flow (%NBR)	$\leq$ Limiting value	Limiting value
Initial Dome Pressure (psia)	1020	1035
Feedwater Temperature	< Max. value	Max. value
Vessel to Relief Vlv Pressure Drop (psi)	Nominal (< 15)	Max. (15)
Vessel to Steam Header Pressure Drop (psi)	< 42.	46.
Control Rod Initial Insertion	Nominal pattern	Minimum scram worth configuration
Control Rod Motion	Rods at different speeds	All rods at same speed (conservative)
CRD Scram Time (seconds to 20% insertion)	Nominal (approximately 0.71)	Tech. spec. upper limit (0.90)
Scram Setpoints.	More conservative than tech. spec.	Tech. spec. limiting value
Protection System Logic Delay (msec)	Nominal (30)	Max. (50)
Number of Relief Vlv's	13	12 (one inoperable)
Relief Vlv Capacity	Nominal	With 0.9 ASME derate
Relief Vlv Setpoint	Nominal	Nominal + 1%
Relief Vlv Response (msec delay/msec stroke)	Nominal (300/100)	Slowest spec. (400/150)
Turb. Stop/Control Vlv Stroke Time (msec)	Nominal (150/250)	Fastest spec. (100/150)
Turb. Bypass Vlv Response (msec to 80% open)	Nominal (200)	Slowest spec. (300)
Recirculation Pump Trip Delay (msec)	Nominal (135)	Maximum spec. (175)
Recirculation Pump Coastdown Constant (sec)	Nominal (4.0)	Conservatively slow (4.5)
Flow Control Mode	Manual	Manual
Controller Settings	Nominal	Nominal
Separator Inertia	Split between inlet & exit junctions	All on inlet junction
Fuel Rod Gap Conductance	Nominal, varying axially & during transient	Conservatively low, uniform axially and constant during transient

to EOC, etc.). As cycle exposure increases, the inventory of partially inserted control rods is reduced and this in turn decreases the rate of scram reactivity insertion. The reduction in scram reactivity insertion rate is the dominant phenomenon for pressurization transients so that the most severe results occur at the maximum cycle exposure.

Near the end of an operating cycle when essentially all control rods are fully withdrawn from the core, the axial power distribution is controlled by the accumulated axial exposure distribution. Since the axial power distribution affects the initial rate of scram reactivity insertion during a transient, the scram reactivity insertion rate is influenced by the exposure distribution used in the analysis. An exposure distribution is utilized in the analyses which produces a conservative scram reactivity insertion rate relative to that of the expected exposure distribution. The target exposure distribution used in the analyses is normally that produced by the power-exposure iteration (reference 6-2) or the so-called "Haling principle" distribution (reference 6-3). However, if the plant operational strategy is expected to result in an exposure distribution more limiting than the Haling distribution, another target distribution conservative relative to the expected operation is used in the analyses.

#### 6.1.2 Initial State Point

The initial power in the model is set consistent with the maximum steam flow capability of 105-percent NBR. A high value of initial steam flow results in a more rapid pressurization and higher maximum pressures. A maximum value of feedwater temperature is utilized along with a nominal 0.2 percent steam carryunder from the separators. The initial reactor dome

pressure is set at 1035 psia which is conservatively high relative to normal plant operation.

The core flow is initialized at the maximum value expected to be utilized by the operating unit. This is normally the rated capacity of 102.5 mib/hr. However, the recirculation system of the Browns Ferry units has the physical capability to produce core flows in excess of the rated capacity at rated power (up to approximately 105 percent of rated flow). The use of the increased flow capability has substantial benefits in simplifying plant operations. For cycles in which use will be made of the increased core flow capability the analyses will be performed for the limiting core flow value.

#### 6.1.3 Scram Reactivity

The dominant conservatism in the licensing basis modeling is in the representation of the rate of scram reactivity insertion. The initial control rod configuration is selected to minimize the rate of scram reactivity insertion (i.e., the minimum use is made of partially inserted control rods consistent with maintaining the power distribution within applicable operating limits). An additional conservatism is inherent in the assumption that all control rods move at the same speed following scram. Use of a uniform speed for all control rods yields a slower initial scram reactivity insertion rate than achieved by a distribution of control rod speeds with the same average motion.

The licensing analysis utilizes the control rod movement versus time following scram solenoid deenergization listed as the upper limit conformance specification on average rod motion in the unit technical specifications (reference 6-4). Table 6-2 shows the assumed rod motion

Table 6-2

Technical Specification Upper Limit on Average Control Rod Motion After Deenergization of Pilot Valve Scram Solenoids

<u>Insertion</u> <u>%</u>	<u>Time</u> <u>(sec)</u>
5	0.375
20	0.900
50	2.000
90	3.500

following scram and has a large degree of conservatism relative to actual measured rod motion data.

#### 6.1.4 Fuel Rod Gap Conductance

The licensing basis core model utilizes a conservatively low fuel rod gap conductance that is uniform axially and constant during the transient. The actual gap conductance tends to be higher in the central areas of the core and the axial power shape tends to shift upwards in the core during pressurization transients increasing the importance of high gap conductance areas. The actual gap conductance is also expected to increase during the transient due to fuel pellet expansion resulting in a further conservatism in the licensing basis model.

#### 6.1.5 Separator Inertia

The effective fluid inertia of the separator is determined from manufacturer's data (reference 6-5) as a function of the separator initial inlet quality. For best-estimate calculations the separator inertia is divided between the separator inlet junction (125) and liquid exit junction (141). The calculations performed for comparison to measured data presented in chapters 3 and 4 used this best-estimate modeling. However, sensitivity studies indicated that the peak transient power and heat flux were insensitive to the inertia of junction 141 but quite sensitive to the separator inlet junction (125) inertia. Since the peak power and heat flux were increased for higher junction 125 inertias, the licensing basis modeling places all of the separator inertia on junction 125 to provide an additional margin of conservatism in the calculation.

#### 6.1.6 Equipment Specifications

The model inputs for equipment performance (e.g., valves, protective system, control system, etc.) are chosen from a combination of expected performance data, conservative equipment design specifications and plant technical specification limits. The plant controller settings do not significantly affect the licensing basis analyses of the limiting pressurization events therefore nominal plant values are employed. Conservative inputs are employed for relief valve opening response and for closure rates for stop, control, and main steam isolation valves. Reactor protection system setpoints and delays are also conservatively set.

#### 6.1.7 Hot Channel Modeling

The hot channel model described in chapter 2 is employed to compute the variation in thermal-hydraulic conditions in the limiting fuel bundle. The transient thermal-hydraulic data is used in evaluating the change in critical power ratio (CPR) via the GEXL correlation (reference 6-6). A standard 1.4 peak design axial power distribution is utilized in the hot channel calculation. The transient variation in normalized bundle power is taken from the RETRAN system model run with 98 percent of the power deposited in the fuel rods and 2 percent deposited directly in the coolant.

The initial hot bundle power and flow are determined as a function of initial CPR by using a steady-state thermal-hydraulics program with a multiple, parallel channel representation of the reactor core, hot fuel bundles, and core bypass paths (reference 6-7). The initial hot bundle power and flow are selected corresponding to an initial CPR (ICPR) which will result in a minimum CPR during the transient within  $\pm 0.02$  of the safety-limit CPR (1.07). Table 6-3 shows the initial conditions for the hot bundle calculation for Browns Ferry unit 3 at EOC 5. The limiting bundle utilized is a GE pressurized 8 x 8 DR design bundle.

Table 6-3

## Hot-Channel Analyses Initial Conditions

<u>Parameter</u>	<u>P8 x 8R Bundle</u>
Radial peaking factor	1.48
Axial peaking factor	1.40
R-factor	1.051
Bundle power (mWt)	6.259
Bundle flow (klb/hr)	107.6
Upper plenum pressure (psia)	1045.2
Inlet enthalpy (Btu/lb)	523.3
Initial MCPR	1.29

## 6.2 Generator Load Rejection Without Bypass

### 6.2.1 Sequence of Events

A loss of generator electrical load from high power conditions produces the approximate sequence of events shown below for the portion of the event important for determining if applicable fuel damage limits have been violated:

- a. Electric load is lost and turbine-generator begins to accelerate (0.000 sec).
- b. The loss of load is sensed by the power-load unbalance (PLU) device which initiates a turbine control valve fast closure to protect the turbine-generator from overspeeding. The imbalance between power and load also generates a signal to open turbine bypass valves but failure to open is assumed (approximately 0.005 sec).
- c. Turbine control valve fast closure is sensed by the reactor protection system which initiates a scram for power levels above 30-percent NBR (approximately 0.035 sec).
- d. Sensed fast control valve closure initiates opening of breakers between recirculation M-G sets and pump motors beginning pump coastdown (approximately 0.180 sec).
- e. Pressure rises to the relief valve setpoints causing them to open and discharge into suppression pool. Flow through the relief valve terminates the pressure increase and begins pressure reduction to the relief valve reclosure setpoint (approximately 1.4 to 7.0 sec).

For the conservative assumptions utilized in the licensing basis analyses, the positive reactivity created by void collapse during the initial reactor vessel pressure rise is sufficient to overcome the negative

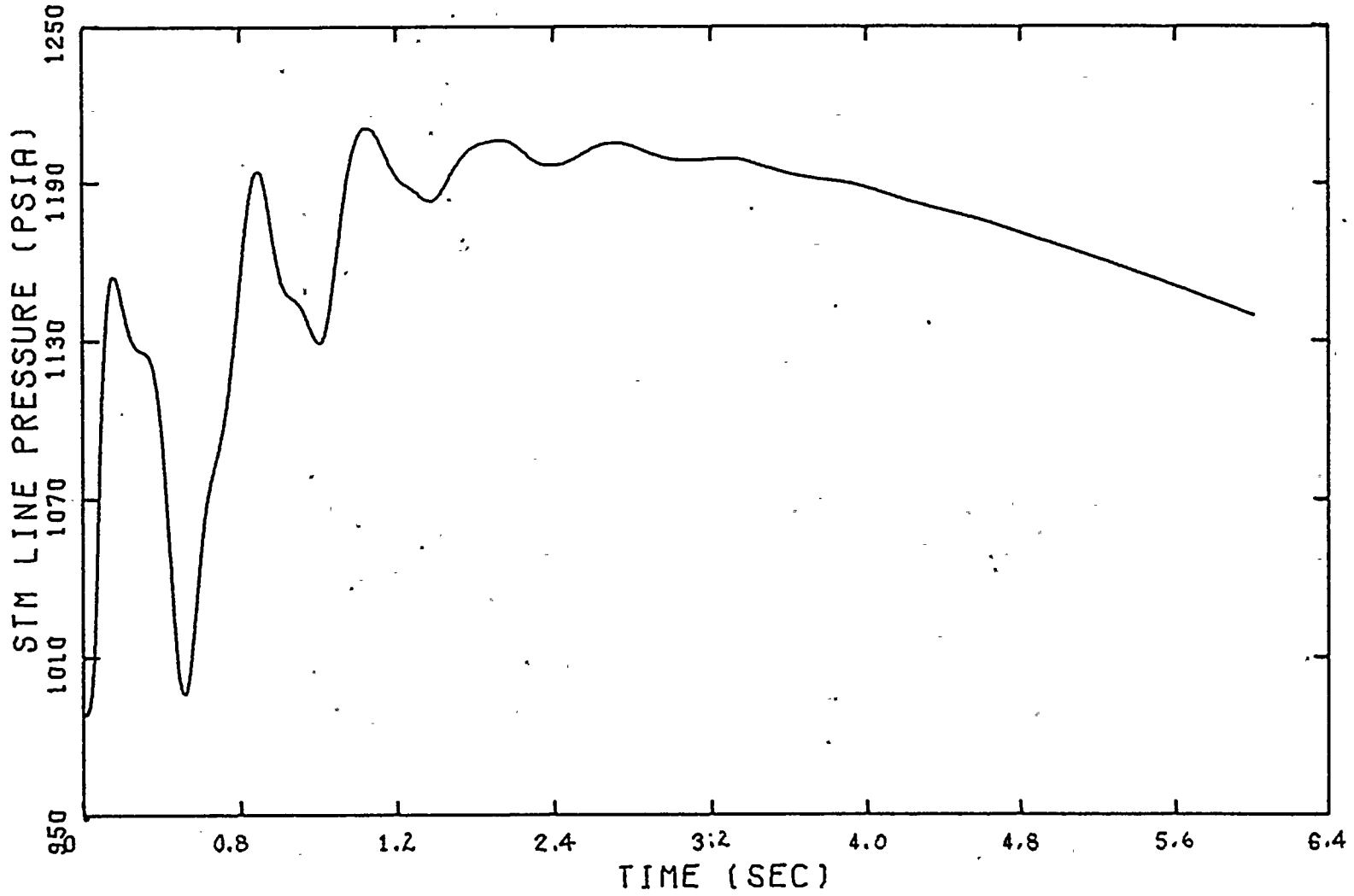
reactivity caused by scram for a short period of time resulting in an increase in reactor power.

### 6.2.2 Results of RETRAN Analysis

The analysis of the GLRWOB for Browns Ferry unit 3 at projected end of cycle 5 conditions was performed with the RETRAN model described in chapter 2 and the licensing basis input as identified in section 6.1. The fast closure of the control valve is simulated by linearly decreasing the flow at fill junction 340 (representing steam flow to the turbine) to zero at 0.075 seconds. This causes a rapid increase in the pressure in the steam line near the turbine as shown in figure 6-1. The pressure disturbance propagates at the speed of sound back to the reactor vessel causing the large oscillations in vessel steam flow shown in figure 6-2. The large negative (i.e., back into the vessel) portion of the vessel steam flow oscillation causes the very rapid pressurization of the reactor dome shown in figure 6-3. The short flat portions of the vessel pressure rise occur when the steam flow oscillation is allowing large positive (i.e., out of vessel) flow rates. The delay in the vessel pressure rise following control valve closure is approximately 0.20 seconds and is determined by the length of the steam lines. The pressures of the core inlet (vessel lower plenum) and core exit (upper plenum) are closely matched and follow the reactor dome pressure. Beyond approximately 0.35 seconds the pressurization rate of the reactor core is causing a net insertion of positive reactivity since the void reactivity is sufficient to overcome the initially very low scram reactivity insertion rate. As shown in figure 6-5

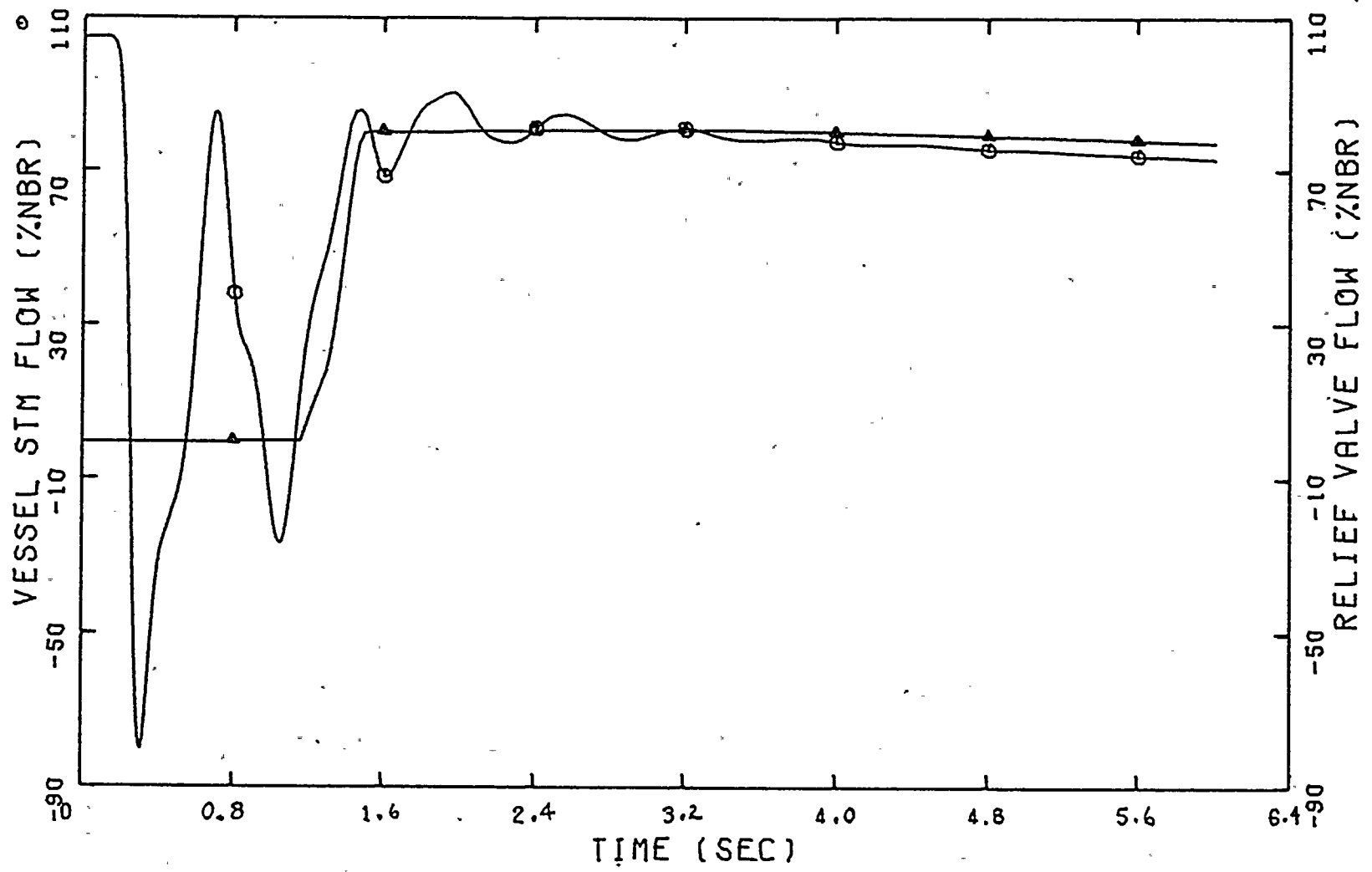
BF3 EOC5 LICENSING BASIS GLRWOB

FIGURE 6-1



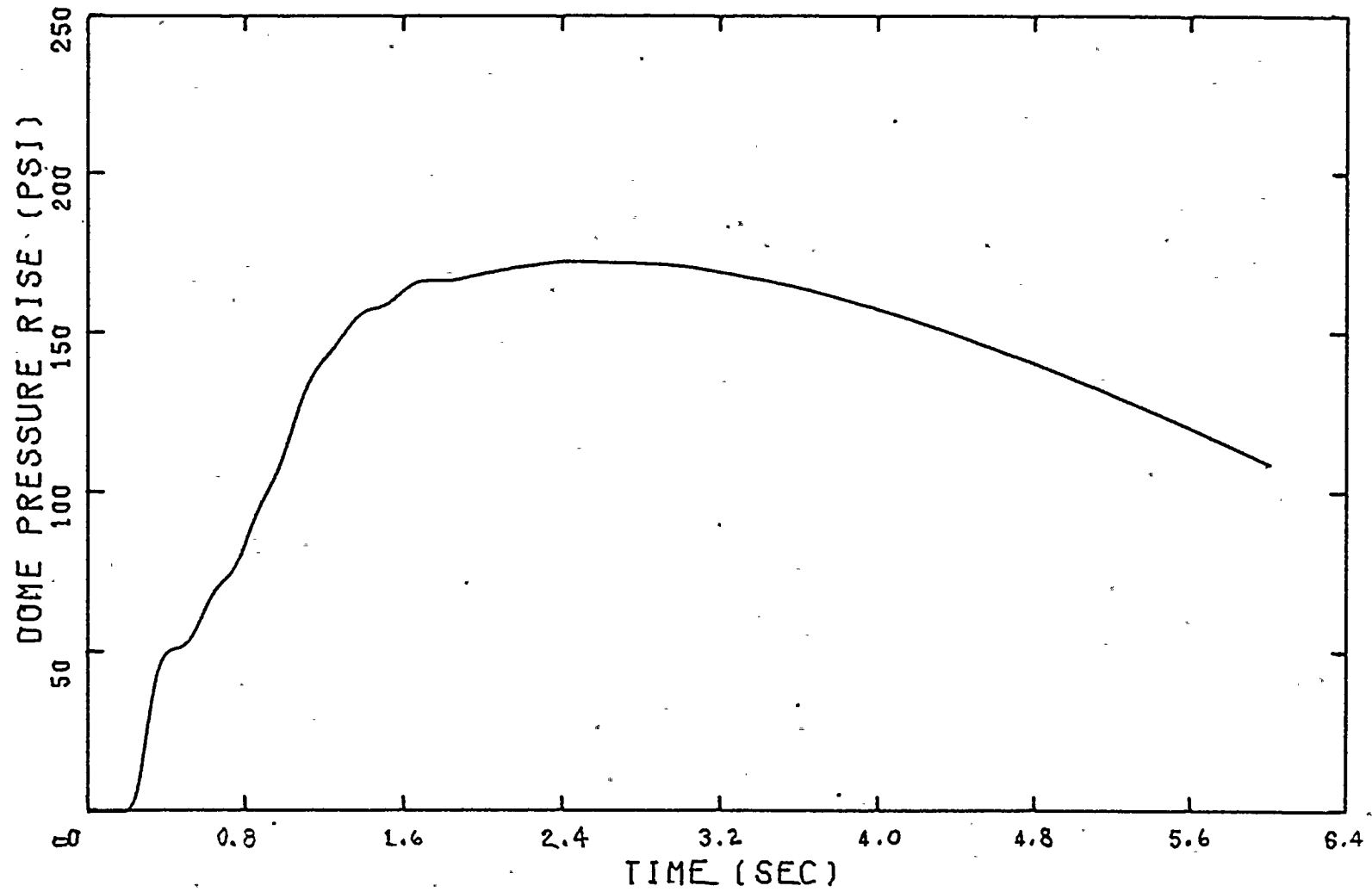
BF3 EOC5 LICENSING BASIS GLRW0B

FIGURE 6-2



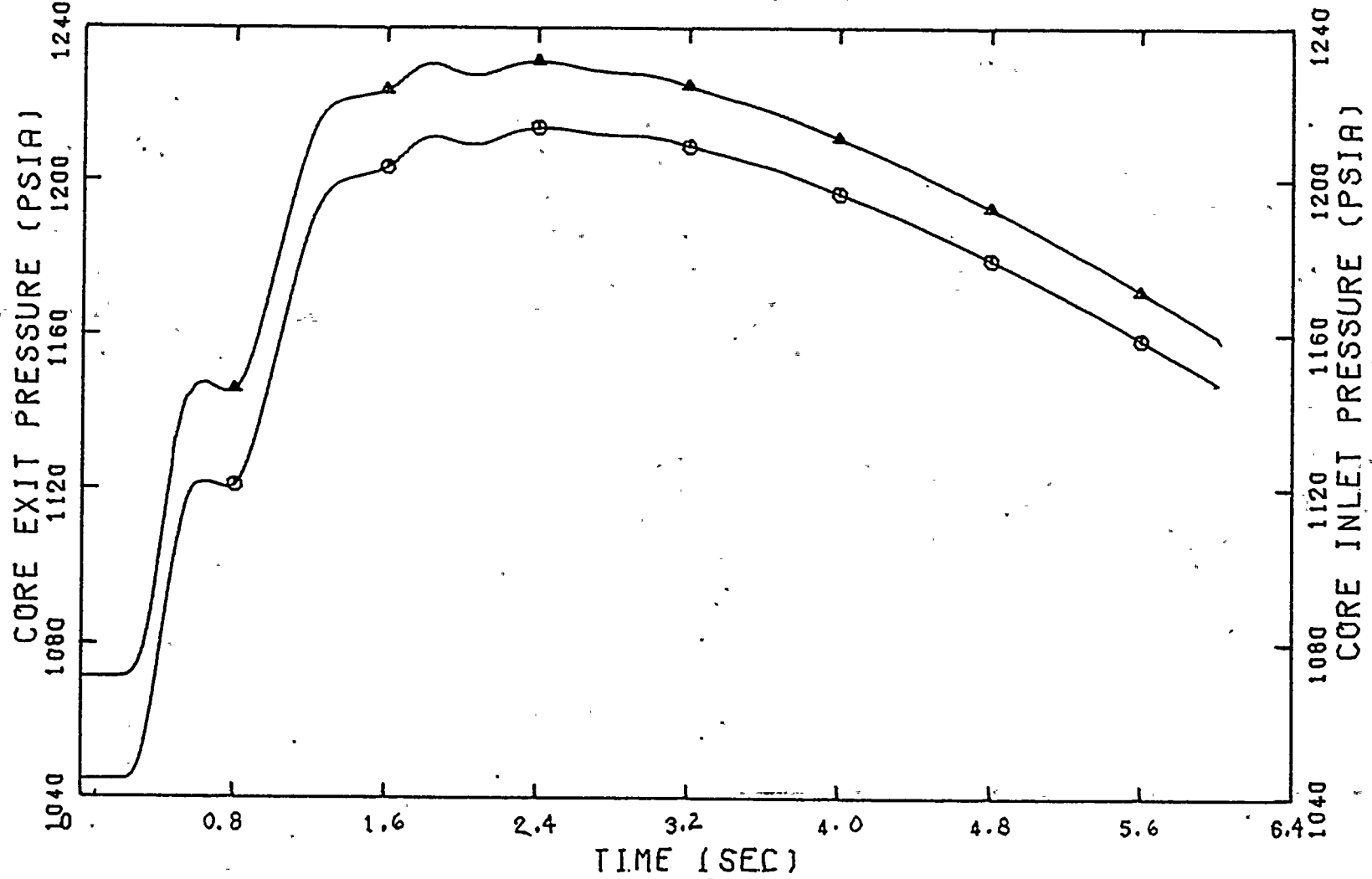
BF3 EOC5 LICENSING BASIS GLRWOB

FIGURE 6-3



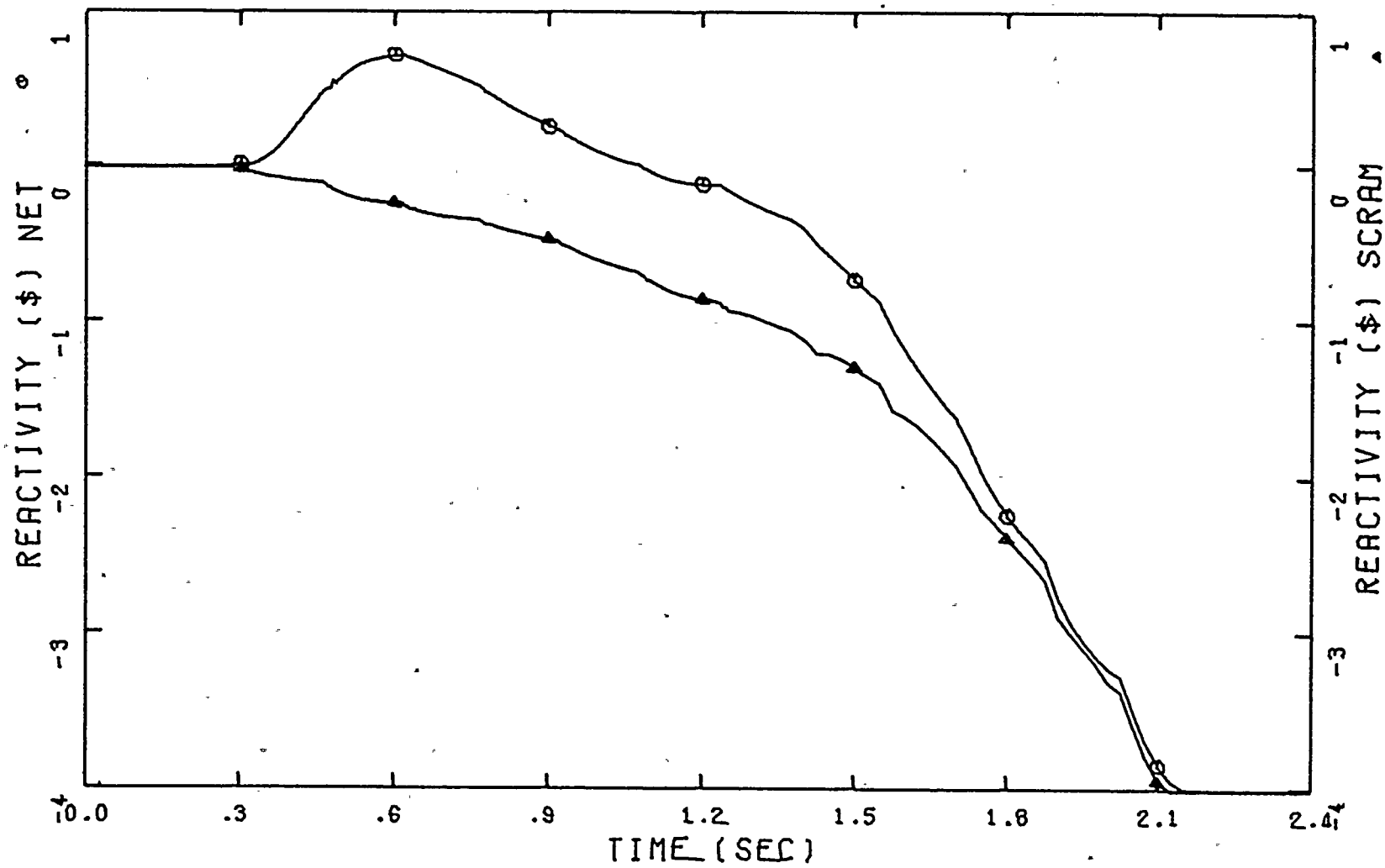
BF3 EOC5 LICENSING BASIS GLRWOB

FIGURE 6-4



BF3 EOC5 LICENSING BASIS GLRWOB

FIGURE 6-5



the net reactivity reaches a maximum of approximately \$0.72 at 0.615 seconds then begins to decrease as negative scram reactivity insertion rapidly increases.

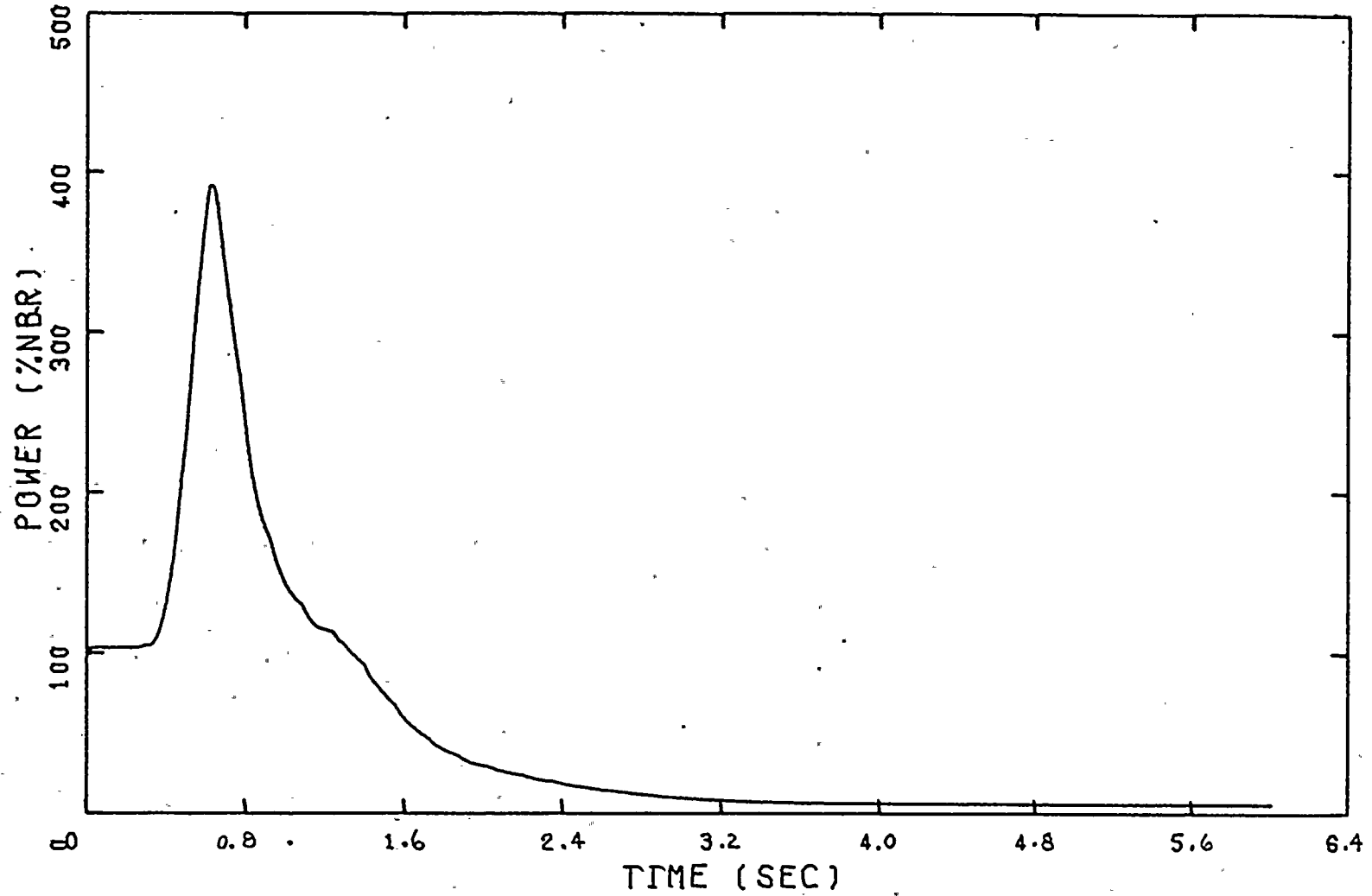
The transient variation in reactor power is shown in figure 6-6. The reactor power rises rapidly to a peak value of 393-percent NBR at 0.63 seconds then rapidly decreases as the scram reactivity terminates the excursion. The behavior of the core average clad surface heat flux during the GLRWOB is shown in figure 6-7. The initial pressure rise in the core causes a reduction in clad-to-coolant heat transfer due to the rise in saturation temperature of the liquid phase. The core average heat flux quickly turns around and begins to rise due to the increased power generation and reaches a peak heat flux of 120.3 percent of the rated steady-state power value at 0.85 seconds then begins to decrease at a rate determined by the reduction in power and the fuel rod time constant.

The core inlet and exit flow rates in figure 6-8 show the compression and expansion oscillations excited by the steam line pressure wave. The magnitudes of the initial core inlet flow increase and core exit flow decrease are influenced by the inertias of the jet pumps and steam separators in addition to the size of the steam line pressure wave.

The feedwater flow and narrow range (NR) sensed level behavior during the GLRWOB are shown in figures 6-9 and 6-10, respectively. The feedwater flow is initially reduced due to the reduced output of the feedwater turbines as the pressure increases. The feedwater flow begins to increase later in the transient as the pressure decreases and the controller demand increases. The NR level transient is relatively mild with a reduction of only 12 inches, leaving a large margin to the MSIV closure setpoint.

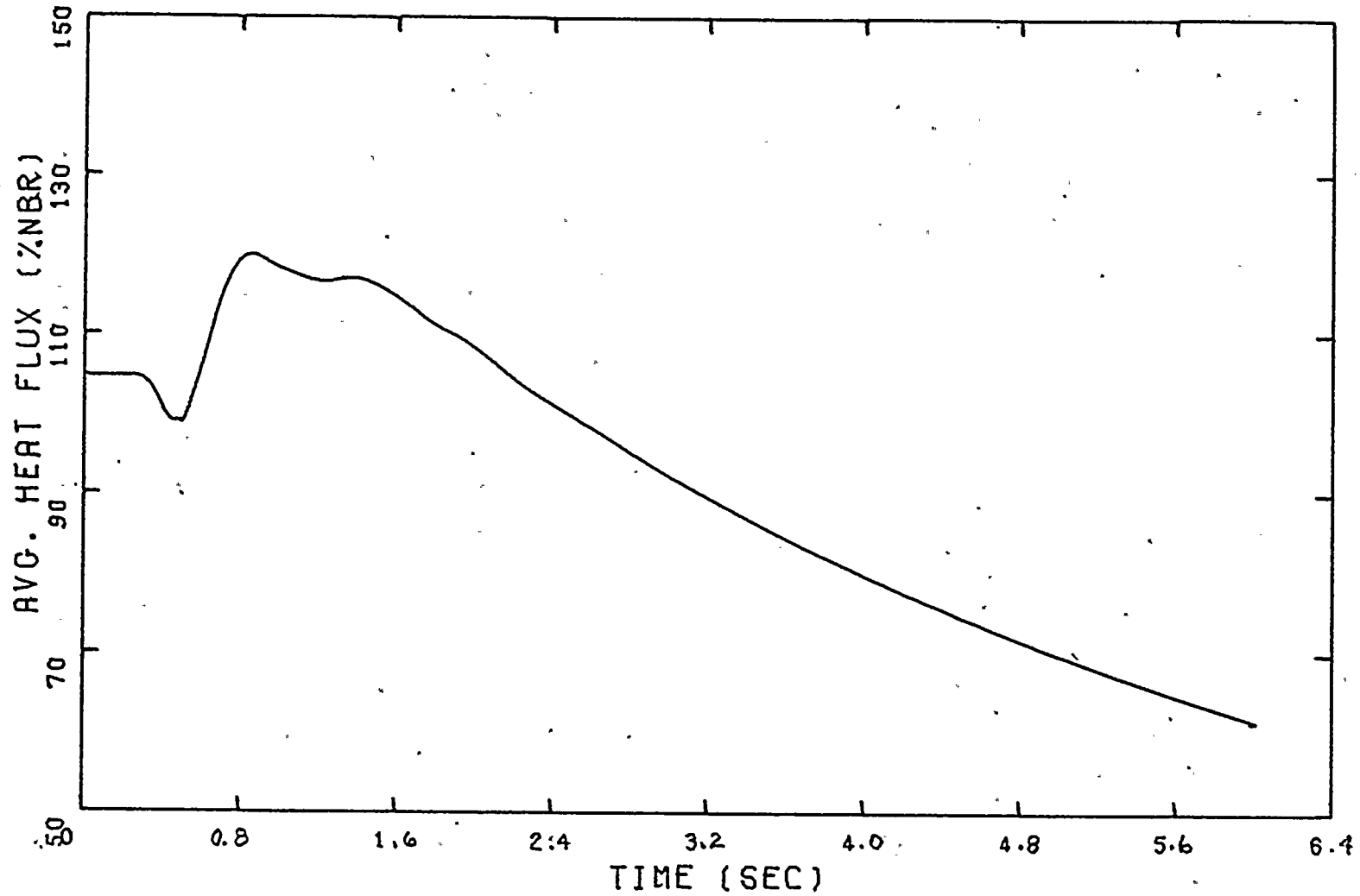
BF3 EOC5 LICENSING BASIS GLRWOB

FIGURE 6-6



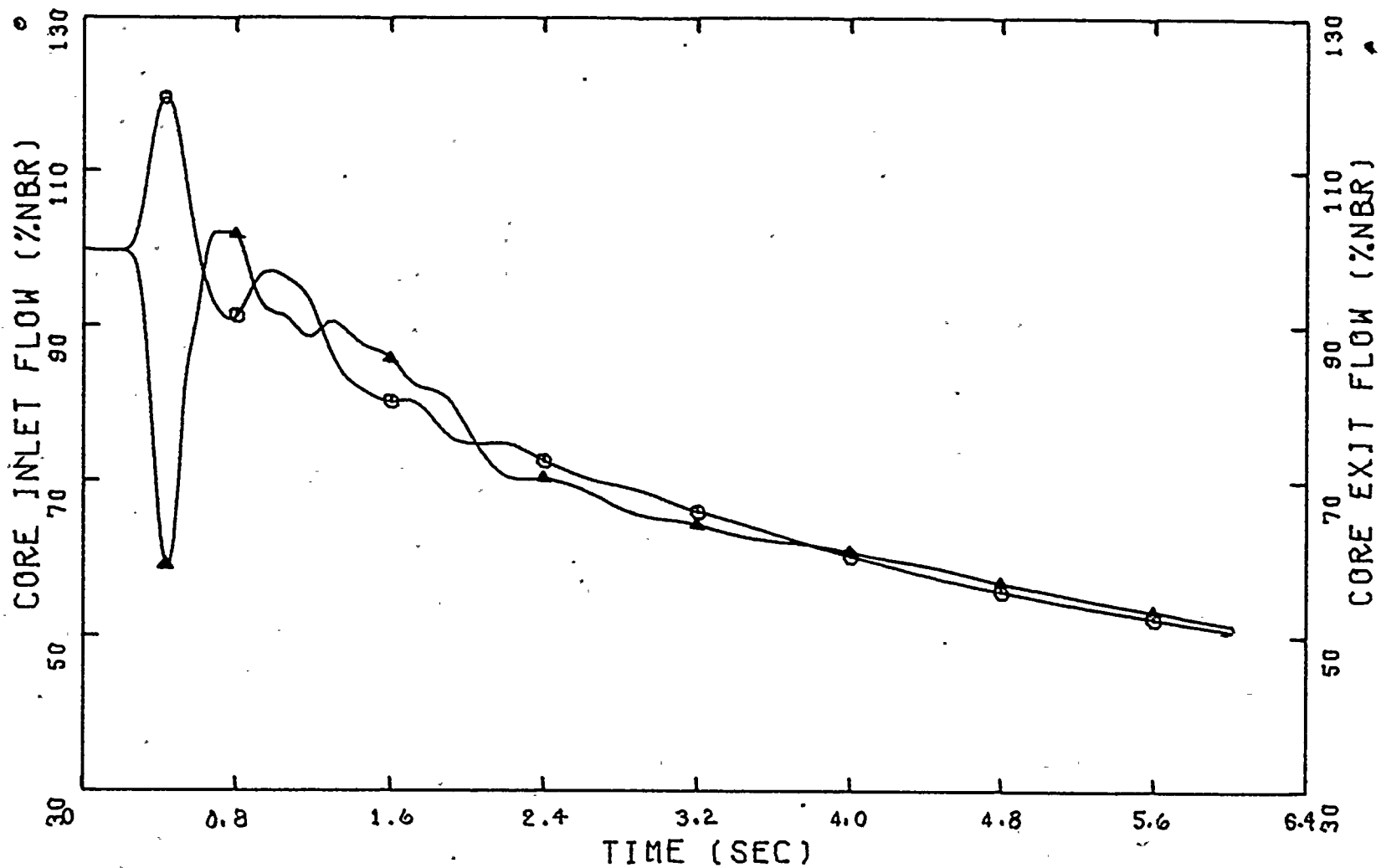
BF3 EOC5 LICENSING BASIS GLRWOB

FIGURE 6-7

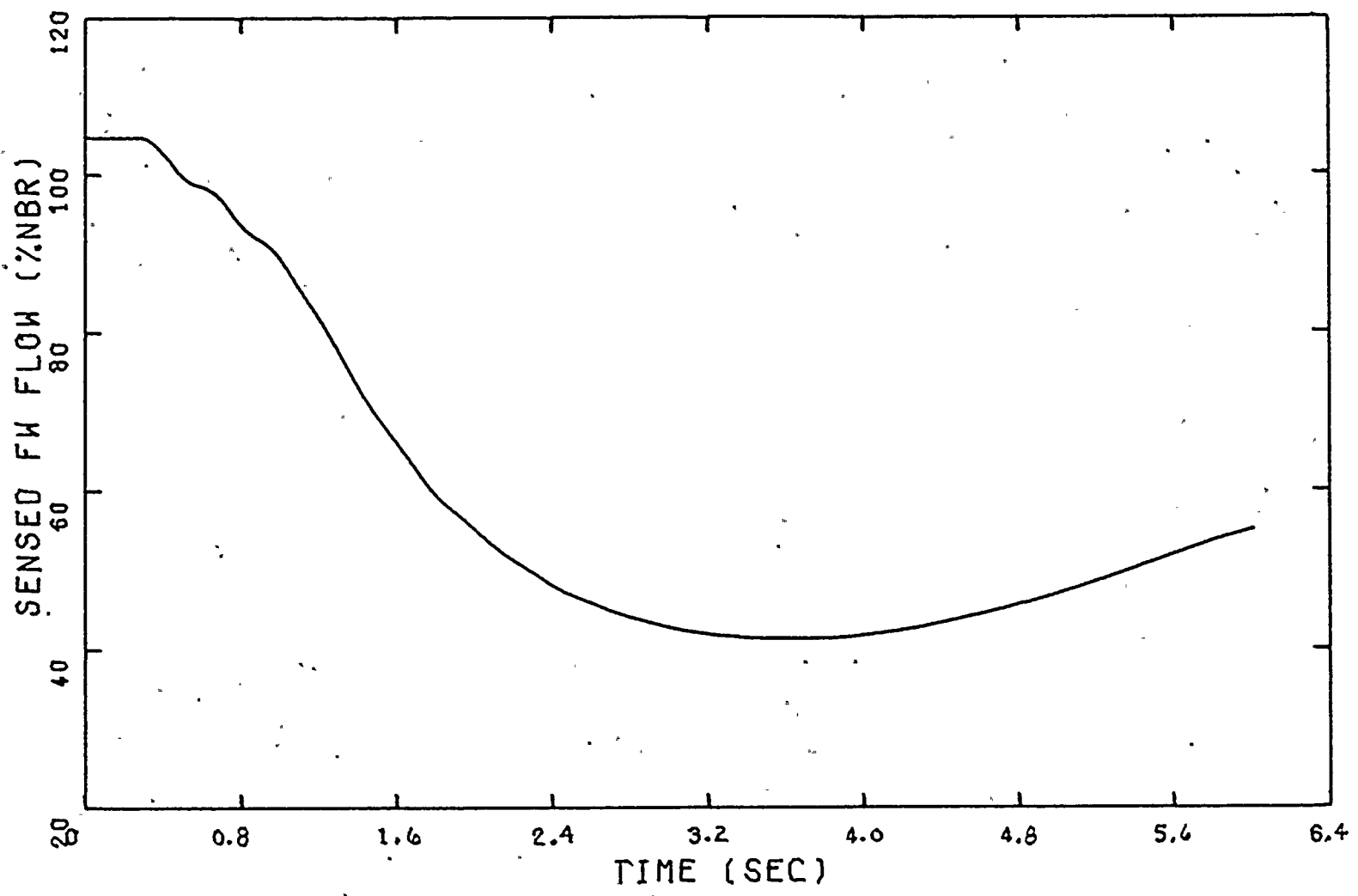


BF3 EOC5 LICENSING BASIS GLRWOB

FIGURE 6-8

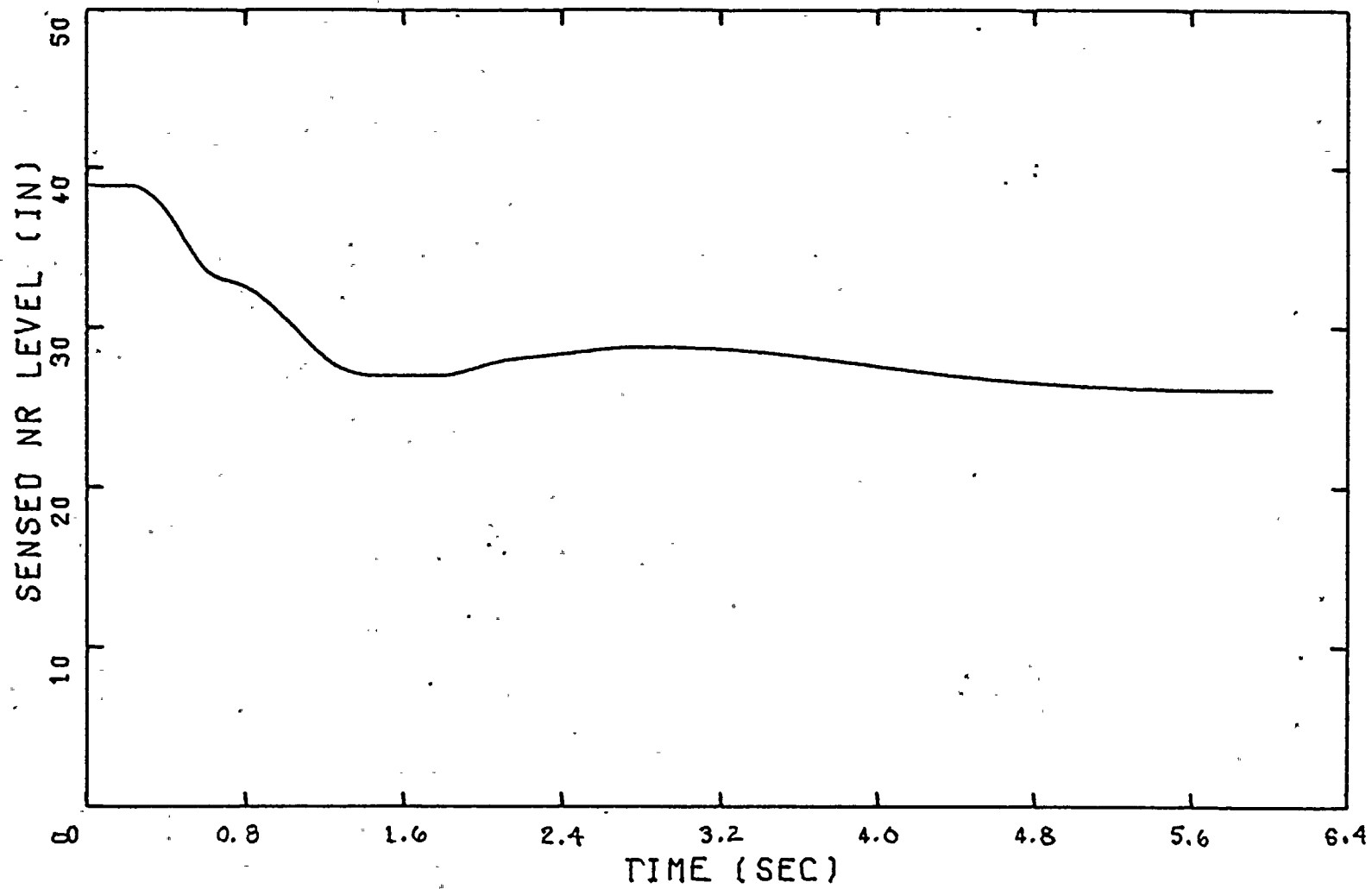


BF3 EOC5 LICENSING BASIS GLRWOB FIGURE 6-9



BF3 EOC5 LICENSING BASIS GLRWOB

FIGURE 6-10



The GLRWOB system transient run was used to provide the time dependent relative power plus thermal-hydraulic boundary conditions for the upper plenum, lower plenum, and core bypass volumes for the hot channel model initialized as discussed in section 6.1.7. The hot-channel run produces time dependent thermal-hydraulic data which is used with the GEXL correlation to compute the change in critical power rates during the event. The minimum CPR calculated was 1.07 and since the initial CPR was 1.29, a value of 0.22 for the  $\Delta$ CPR for the GLRWOB was obtained.

### 6.3 Feedwater Controller Failure (FWCF)

This event is postulated on the basis of a single failure of a control device, specifically one which can directly cause an increase in coolant inventory by increasing the feedwater flow. The most severe applicable event is a FWCF to a maximum demanded flow output. The peak pressure, power, and heat flux values are largest when the event is initiated from maximum power and steam flow. However, the relative increase in power and heat flux may be larger at the lower end of the flow control range since this generates a large increase in feedwater flow and a correspondingly greater reduction in inlet subcooling. The improvement in the initial scram reactivity insertion rate due to either the axial power shape shift towards the bottom of the core (for decreases of power along a flow control line) or due to initially inserted control rods (for operations below the maximum power flow lines) is generally sufficient to cause the reduced initial power FWCF operating limit CPR to be bounded by that obtained for maximum power conditions. Even neglecting the improvement in scram reactivity insertion rate, the consequences of the FWCF at reduced flow operation is conservatively bounded by the maximum power results when corrected by the applicable  $K_f$  curve (reference 6-4) for core flow below 75 percent of rated.

The change in  $\Delta\text{CPR}$  for the FWCF event is slightly more severe for feedwater enthalpies less than the maximum value as shown in chapter 7. To account for the potential slight nonconservatism in the licensing basis conditions for the FWCF a penalty of 0.03 is added to the RETRAN model  $\Delta\text{CPR}$  results. This penalty is significantly larger than the potential changes due to uncertainties in feedwater temperature or due to initial power level.

### 6.3.1 Sequence of Events

The analysis of the FWCF event is based on the assumptions and sequence of events listed below.

- a. With reactor operating in manual flow control mode (which results in most severe transient), feedwater controller is assumed to fail to a maximum demanded output (0.0 sec).
- b. Feedwater turbines accelerate at maximum rate to maximum runout capability (approximately 3.0 sec).
- c. Excess in feedwater flow results in an increase in core inlet subcooling which in turn causes a rise in core power (approximately 9.0 sec).
- d. Feedwater flow increase creates a mismatch with steam flow which eventually increases vessel water level to high water level turbine trip setpoint (15.5 sec).
- e. High water level causes tripping of feedwater pumps and turbine trip (15.5 sec).
- f. Turbine trip initiates reactor scram and closure of stop valves begins pressure increase (approximately 15.53 sec).
- g. Turbine trip signal initiates opening of RPT breakers beginning pump coastdown (15.675 sec).

- h. Increase in steam line pressure causes turbine bypass valves to open (approximately 15.80 sec).
- i. Pressure rises to setpoint of relief valves which open, terminating the pressure increase and begins pressure reduction to relief valve reclosure pressure (approximately 17.15 to 20.0 sec).

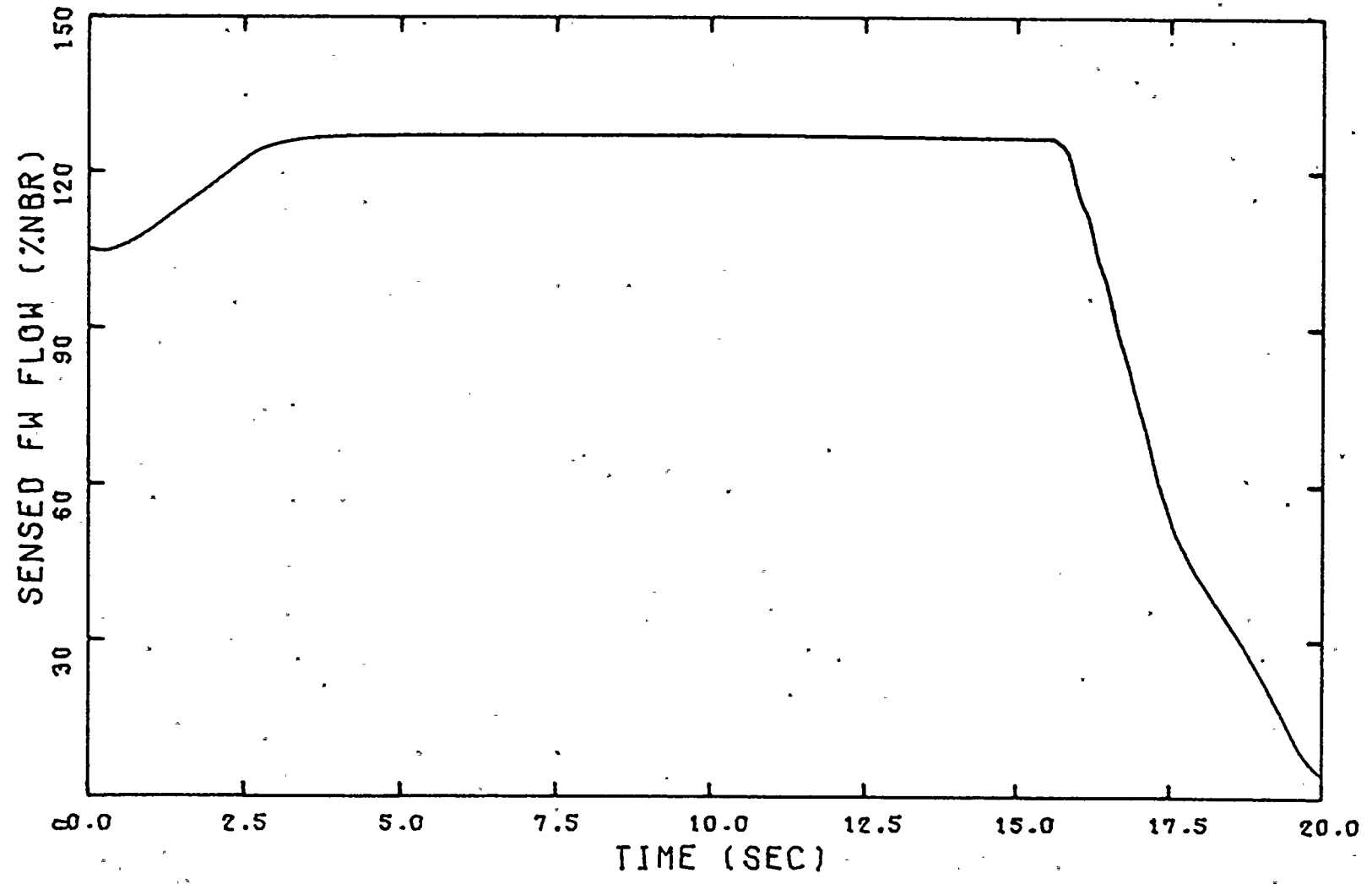
As can be seen from the above sequence of events, the FWCF evolves into a turbine trip with bypass event from a higher than initial power level and lower inlet temperature.

### 6.3.2 Results of RETRAN Analysis

The FWCF event was analyzed for the initial conditions previously described and was initiated by setting the output of the feedwater controller to its maximum output. The resulting feedwater flow is shown in figure 6-11. The increase in feedwater flow decreases the average temperature in the mixing downcomer and after the transport time through the lower downcomer (approximately two-thirds of flow) and recirculation loops (approximately one-third of flow) causes an increase in the core inlet subcooling as in figure 6-12. The excess feedwater flow also causes the reactor water level to increase as shown in figure 6-13. The NR sensed water level reaches the high level turbine trip setpoint at approximately 15.5 seconds causing a turbine trip. Closure of the stop valves causes the pressure to increase. Part of the steam flow is relieved by opening of the turbine bypass valves (figure 6-14) but for high initial power levels the bypass capacity is not sufficient to prevent further reactor pressure increases as shown in figure 6-15. For the conservative assumption of the licensing basis analysis, the positive reactivity from core pressurization following the turbine trip is initially sufficient to overcome the negative scram reactivity insertion (figure 6-16) and a rapid increase in power

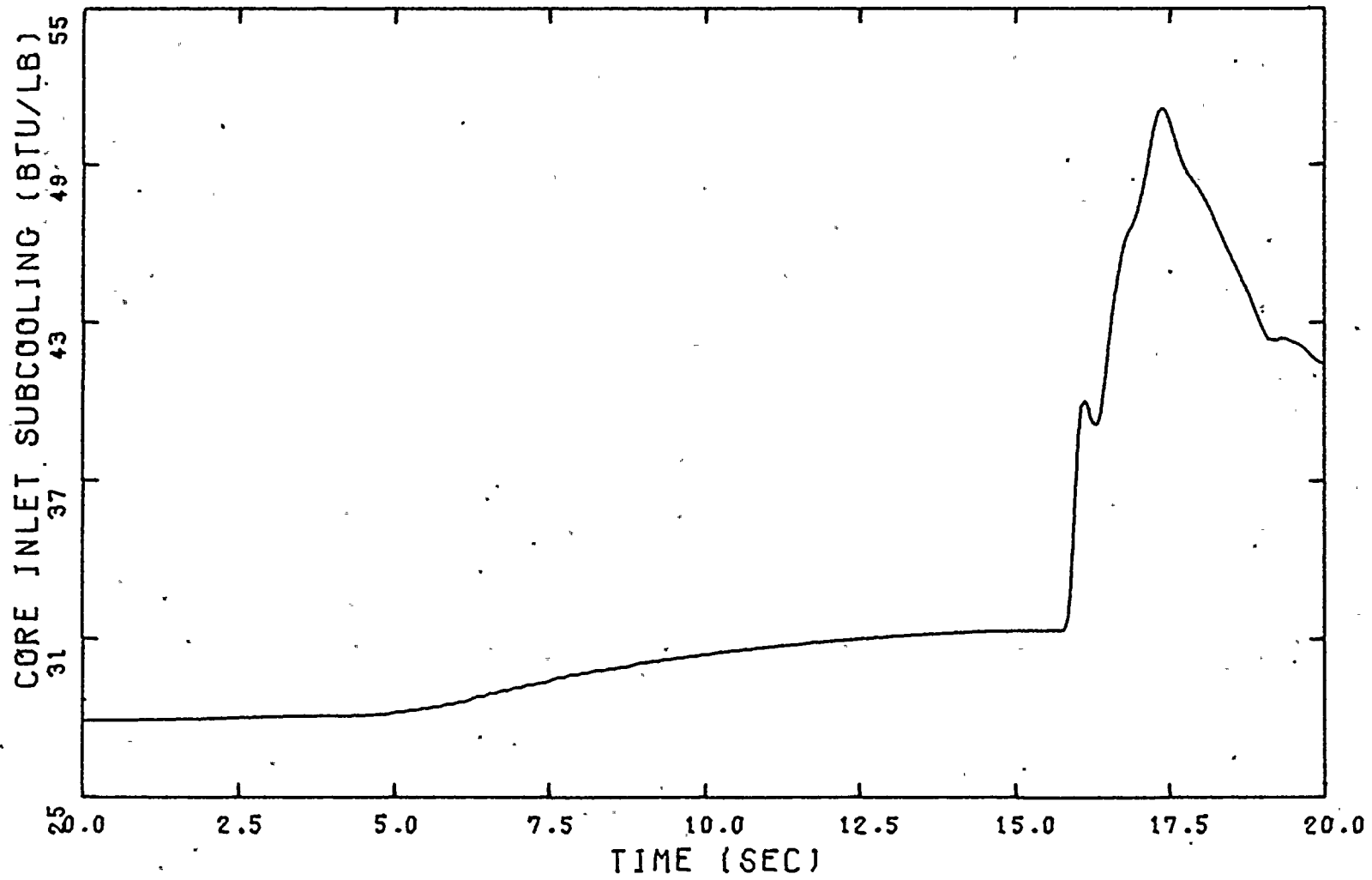
BF3 EOC5 LICENSING BASIS FWCF

FIGURE 6-11



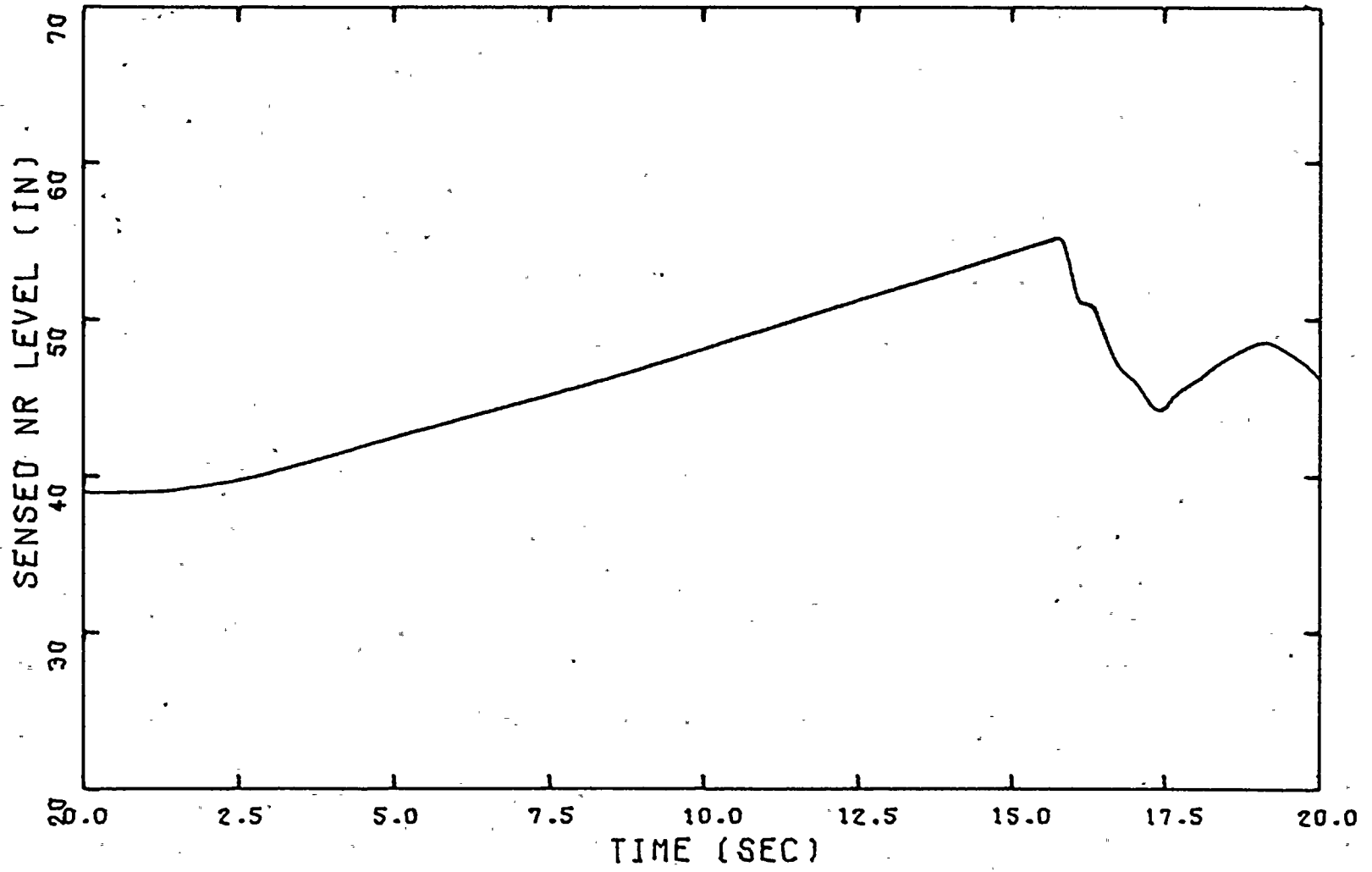
BF3 EOC5 LICENSING BASIS FWCF

FIGURE 6-12



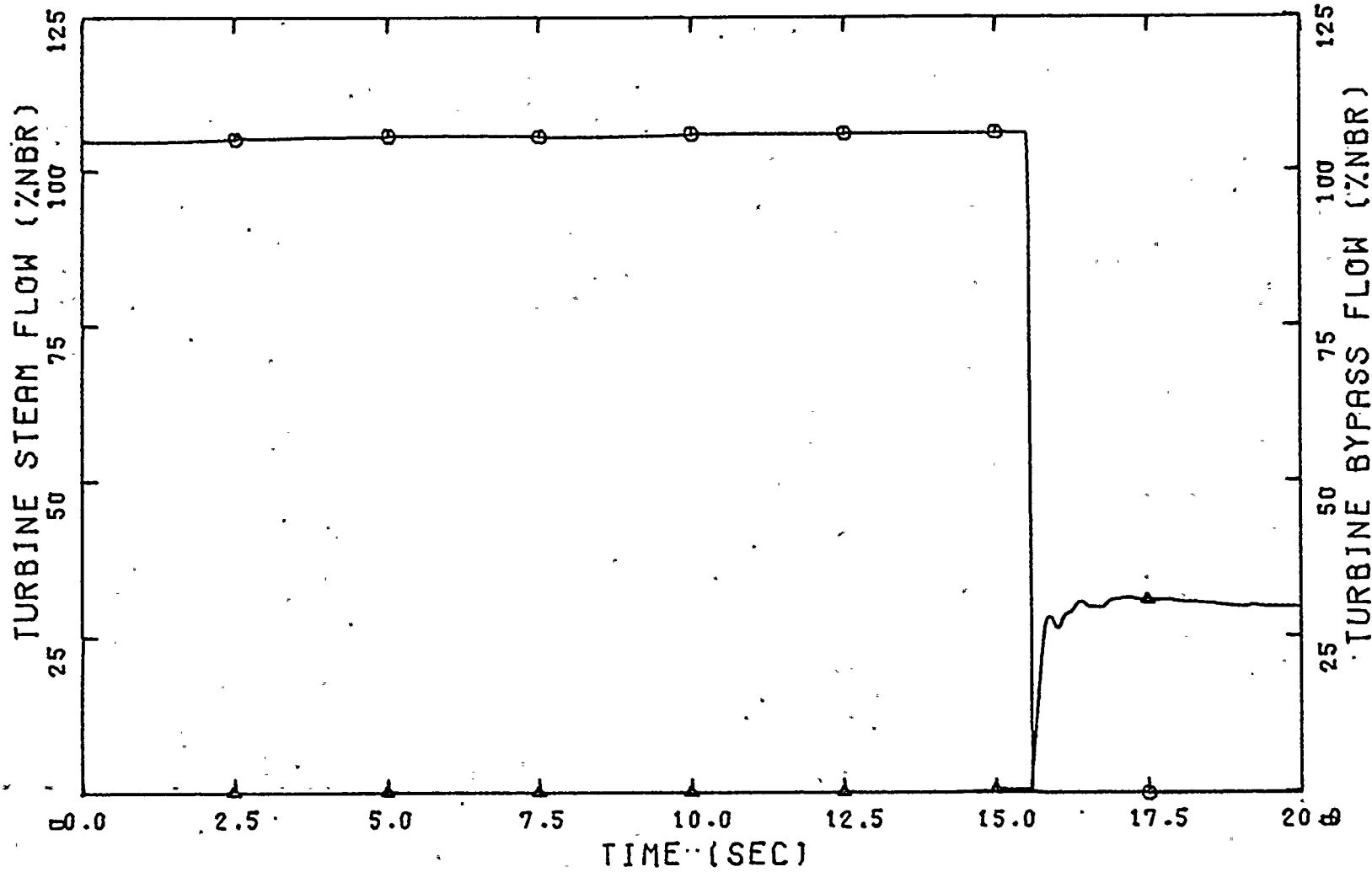
BF3 EOC5 LICENSING BASIS FWCF

FIGURE 6-13



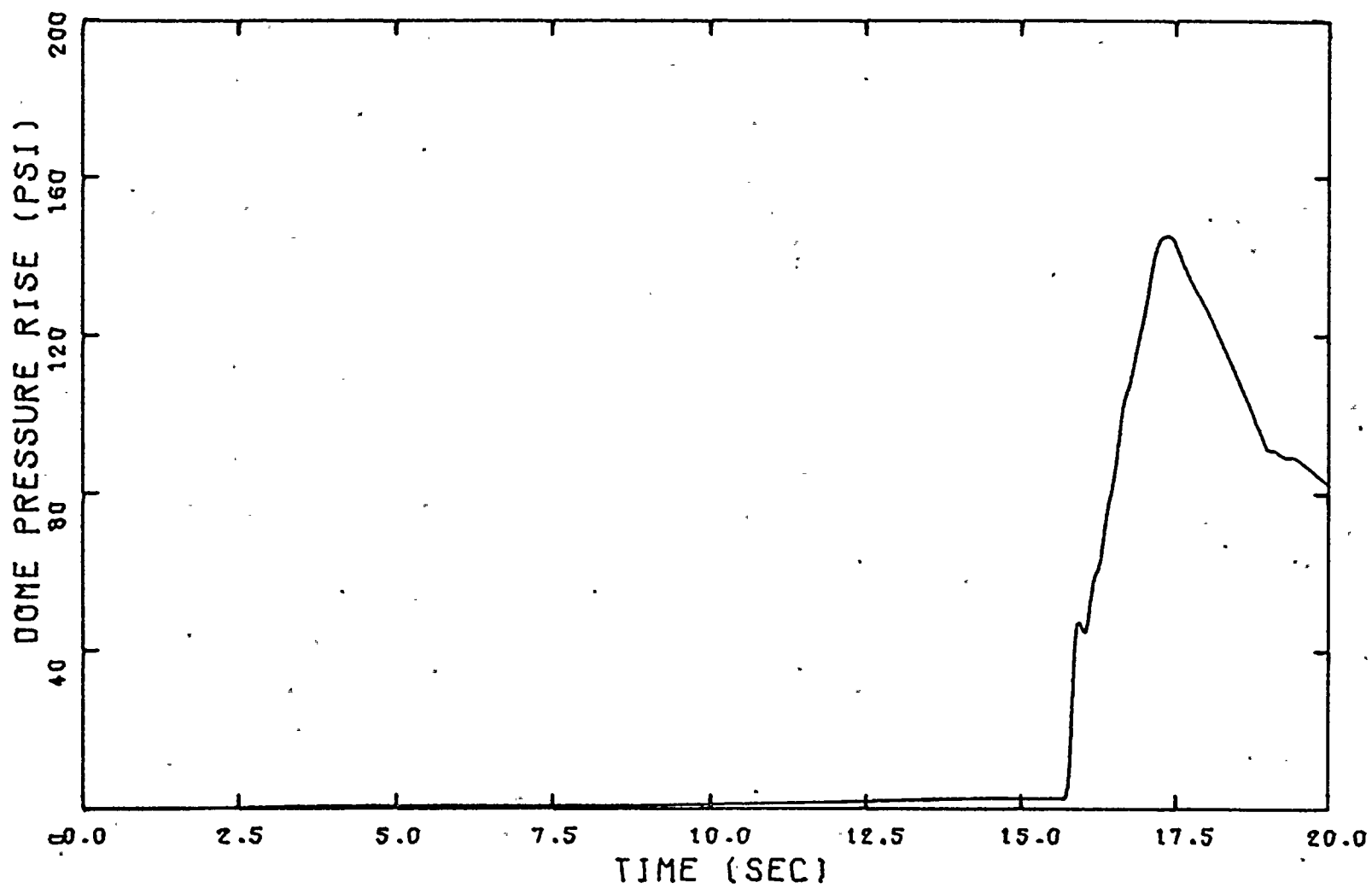
BF3 EOC5 LICENSING BASIS FWCF

FIGURE 6-14



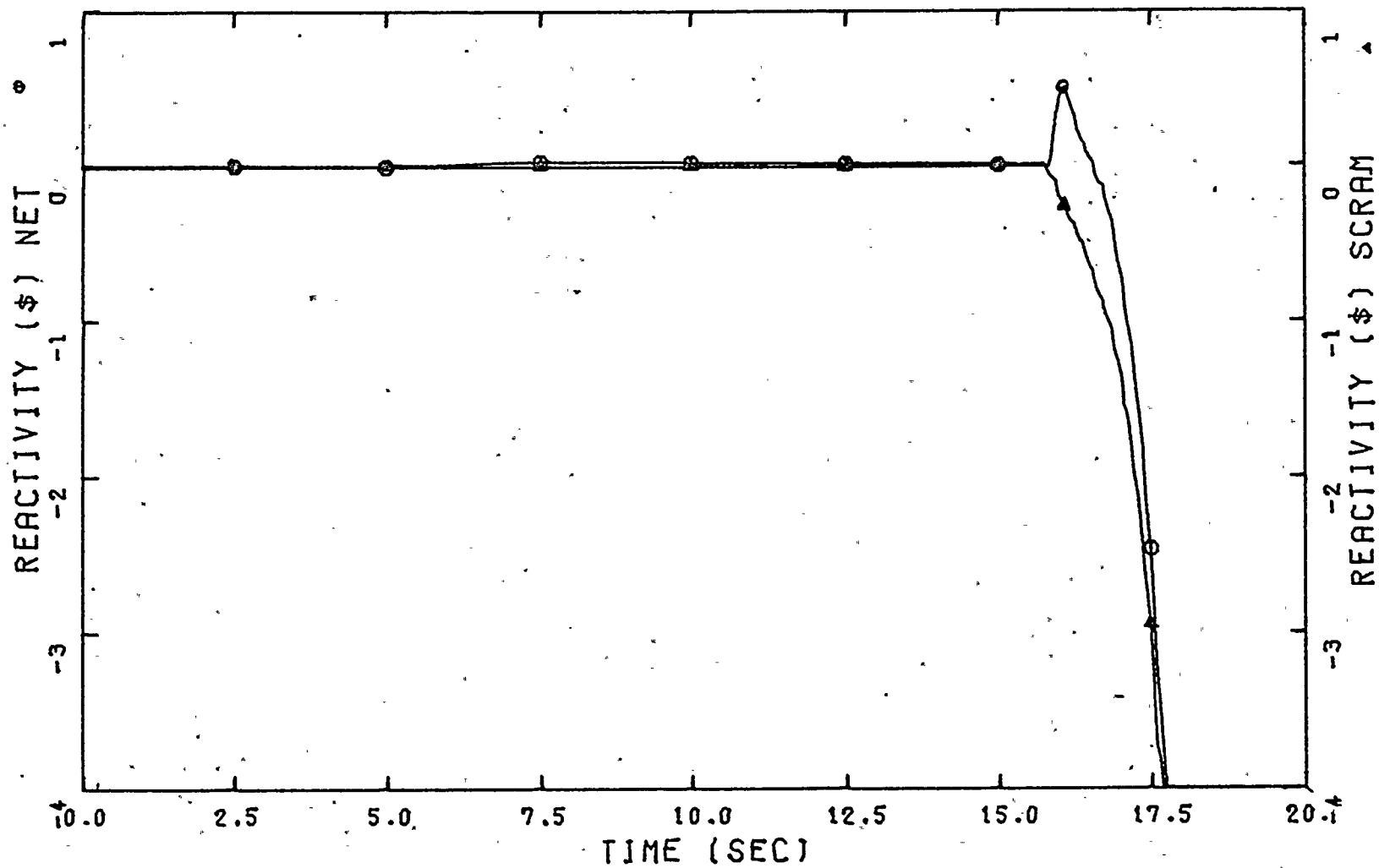
BF3 EOC5 LICENSING BASIS FWCF

FIGURE 6-15



BF3 EOC5 LICENSING BASIS FWCF

FIGURE 6-16



occurs (figure 6-17). The increase in reactor power causes an increase in core average heat flux as depicted in figure 6-18.

The pressure continues to increase until the relief valves open and additional steam flow is relieved to the torus (figure 6-19). The closure of the stop valves generates an oscillation in the vessel steam flow also shown in figure 6-19. The pressure wave excites the oscillation in core inlet and exit flows shown in figure 6-20. The overall reduction in core flow near the end of the simulation is due to the coastdown of the recirculation pumps following the opening of the RPT breakers.

The power excursion is eventually terminated by the scrammed control rods and the pressure rise is reversed by the turbine bypass and relief valves. Over the longer term (portion of the event not simulated) the reactor level will be reduced since the feedwater pumps have been tripped and eventually the level will be maintained by the HPCI/RCIC systems.

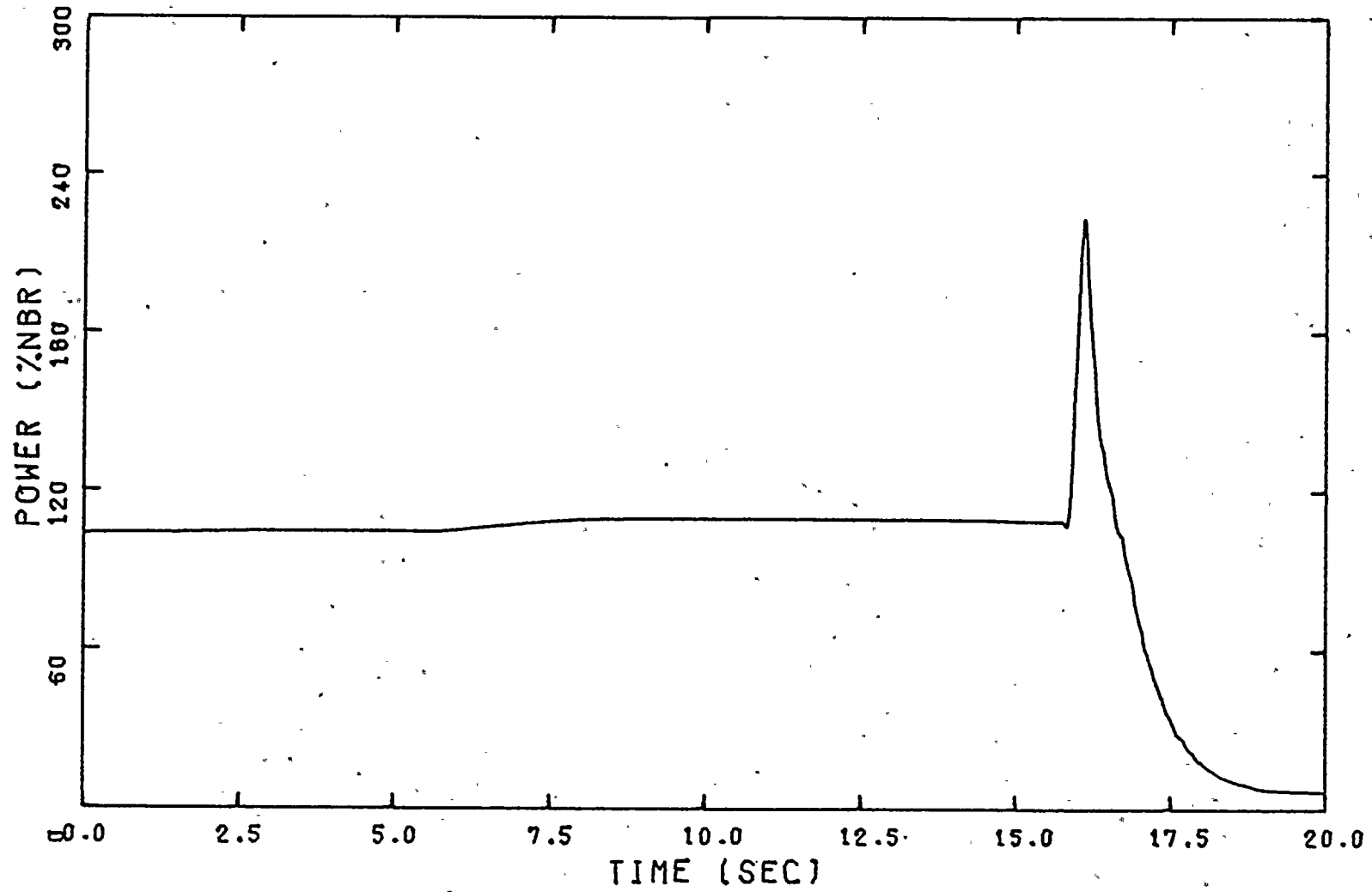
The hot-channel model was utilized with boundary conditions from the FWCF system run (as previously described for the GLRWOB) to determine the transient variation in critical power ratio. For the initial hot-channel conditions listed in table 6-3, a  $\Delta$ CPR of 0.14 was obtained for the FWCF event and adjusted to 0.17 as described in section 6.3.

#### 6.4 Main Steam Isolation Valve Closure with Flux Scram (MSIVC)

The simultaneous closure of all main steam isolation valves with indirect scram on high power or flux (direct scram on MSIV position disabled) event was selected by the Browns Ferry Nuclear Steam Supply System vendor as a conservative basis for analyzing compliance with ASME Boiler and Pressure Vessel Code for "upset" conditions. The boiler and pressure vessel code defines four categories of conditions for overpressure protection system design: (1) normal, (2) upset, (3) emergency, and

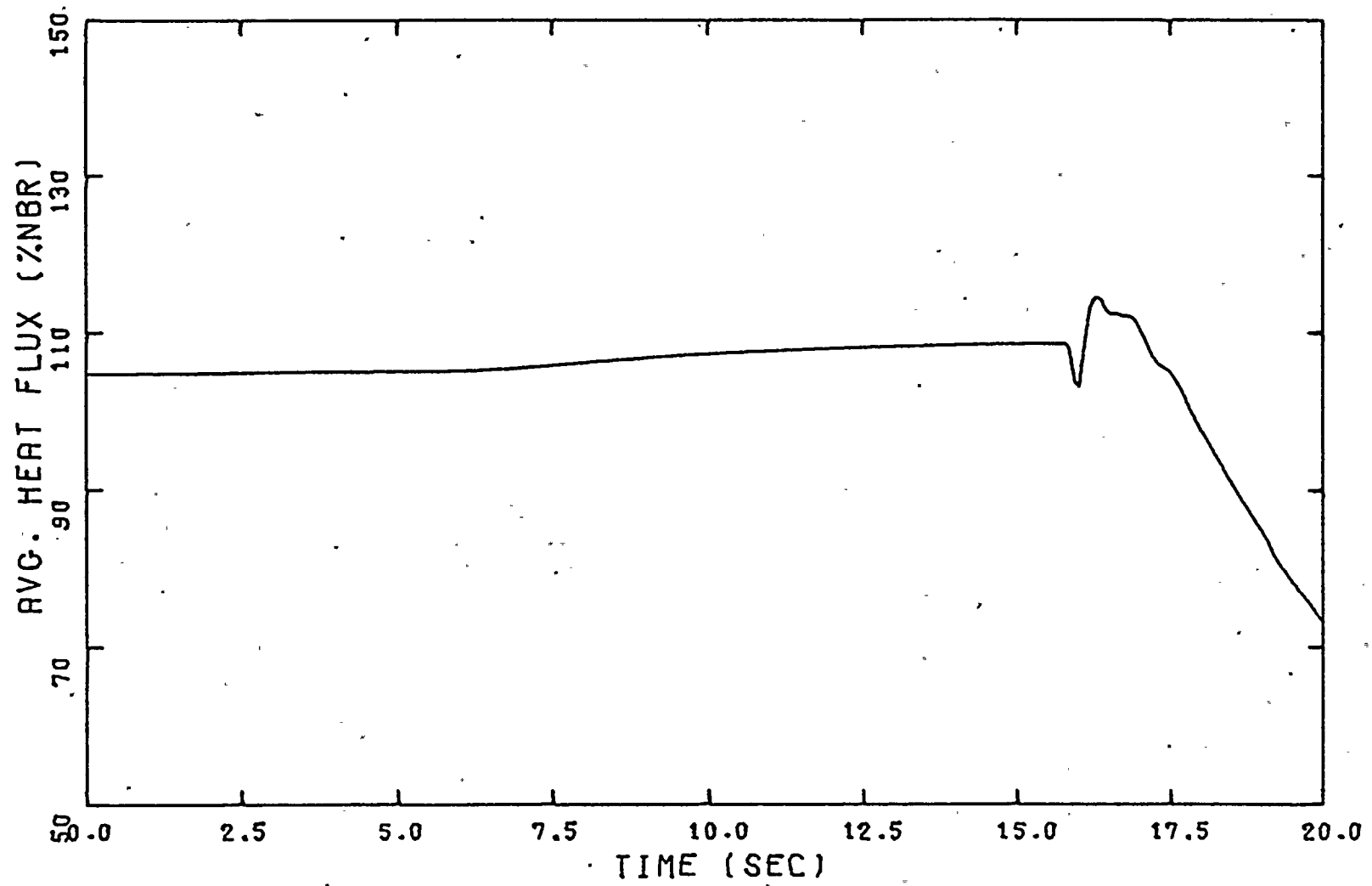
BF3 EOC5 LICENSING BASIS FWCF

FIGURE 6-17



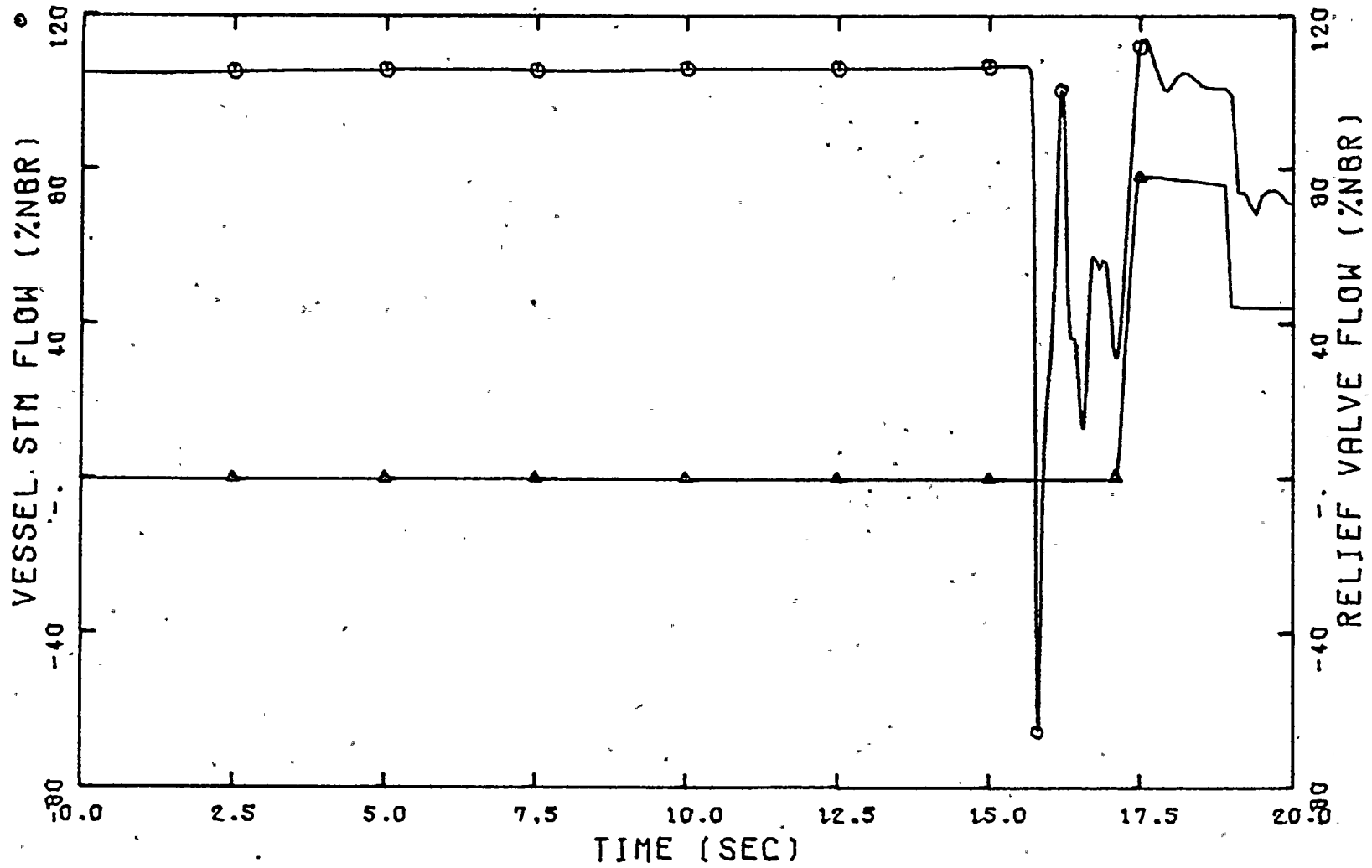
BF3 EOC5 LICENSING BASIS FWCF

FIGURE 6-18



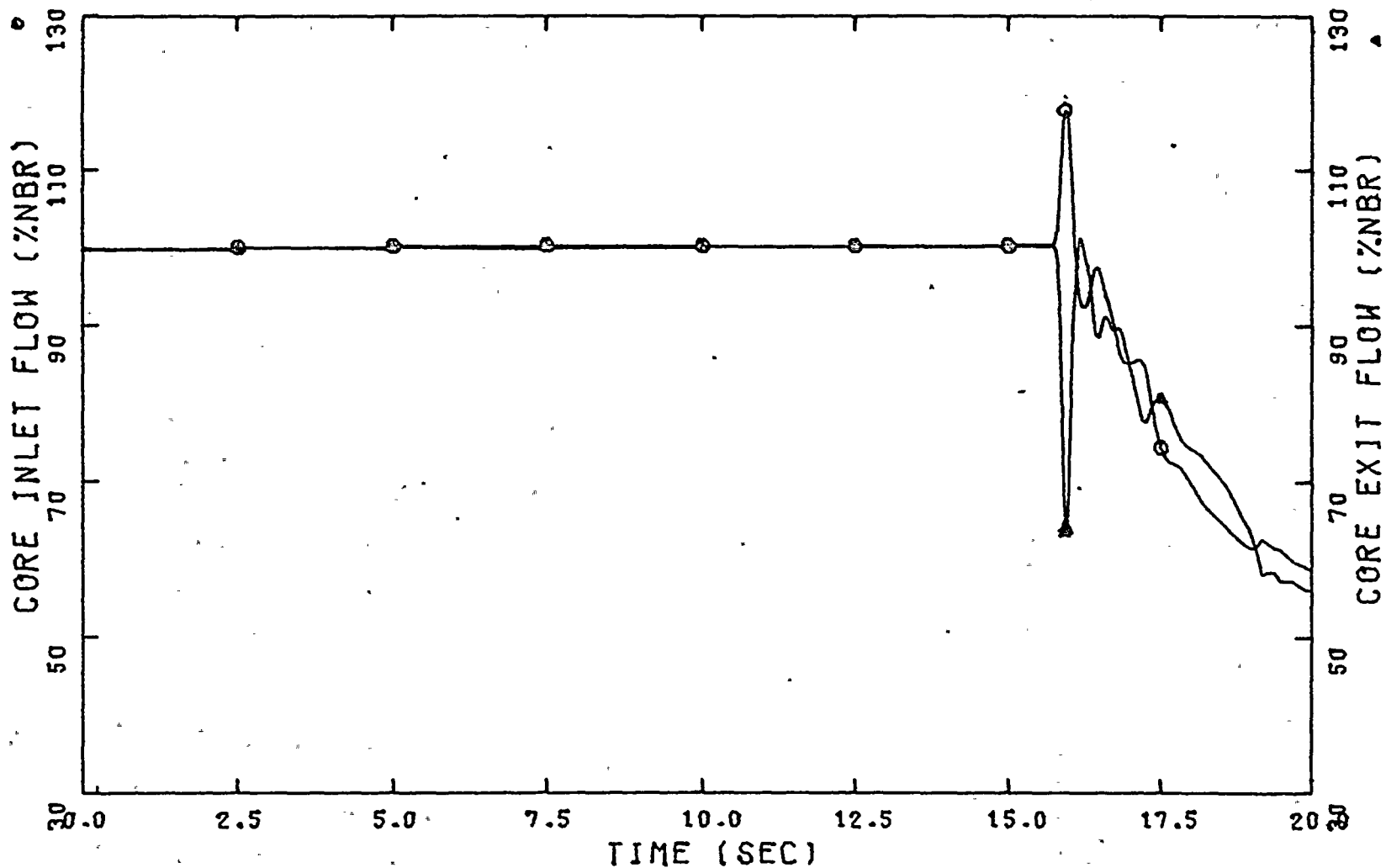
BF3 EOC5 LICENSING BASIS FWCF

FIGURE 6-19



BF3 EOC5 LICENSING BASIS FWCF

FIGURE 6-20



(4) faulted. The compliance criteria for upset conditions is that the maximum vessel pressure not exceed 110 percent of the design pressure (for Browns Ferry  $1.1 \times 1250 = 1375$  psig). Based on the probability of occurrence the MSIVC flux scram event could reasonably be placed in the "emergency" condition category and thus provides a conservative basis for testing of compliance with upset condition limits. The maximum pressures for emergency and faulted conditions are 1500 and 1875 psig, respectively and analyses by the NSSS vendor have previously established these limits to be far less restrictive than the analysis of MSIVC flux scram event under upset conditions.

The MSIVC with indirect scram has a probability of occurrence far below that considered for abnormal operational transients and thus is not considered in determining the operating limit CPR. The MSIVC event with direct scram on valve position has consequences bounded by the GLRWCB and thus analysis for each reload is not required.

#### 6.4.1 Sequence of Events

The main steam isolation valves on all four main steam lines are assumed to close simultaneously at the fastest rate allowed by plant technical specifications (3 sec) and a conservative nonlinear valve closure characteristic is assumed. With the direct scram on MSIV position disabled the approximate sequence of events shown below occurs.

- a. Isolation trip initiates closure of MSIVs (0.0 secs).
- b. Sensed APRM signal reaches 120 percent of initial value and initiates reactor scram (1.75 sec).
- c. Control rod motion begins and slows rate of increase of power (2.04 sec).

- d. Worth of scram reactivity becomes larger than positive reactivity from void collapse and power increase is terminated (2.2 sec).
- e. Pressure reaches lowest setpoint of relief valves and 3 of 4 in the group open (1 assumed failed). The remaining relief valve groups open as pressure reaches their setpoints (2.82 sec).
- f. MSIVs are fully closed (3.0 sec).
- g. High pressure causes tripping of M-G sets and coastdown of M-Gs and pumps begins (3.28 sec).
- h. Maximum pressure is reached in reactor vessel and pressure begins decreasing (approximately 3.9 sec).

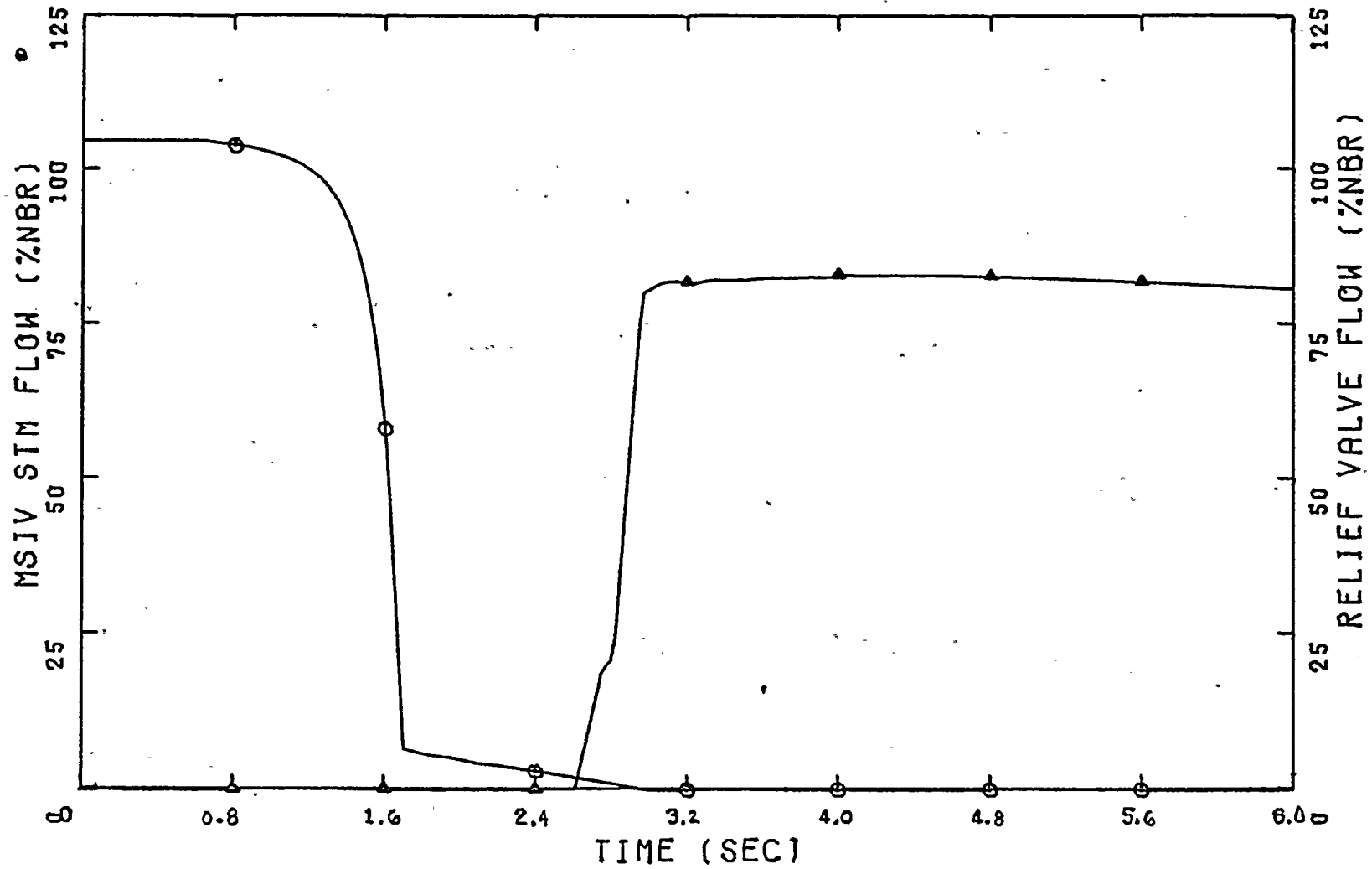
The times for many of the items in the above sequence of events apply to the RETRAN analysis presented in the next section and the times are dependent upon reload specific kinetics data and setpoints.

#### 6.4.2 Results of RETRAN Analysis

The steam flow rate through the closing MSIVs is shown in figure 6-21 along with the relief valve flow. The highly nonlinear closure characteristic assumed for the MSIVs results in the MSIV flow being largely shut off by 1.7 seconds. The rapid reduction in MSIV flow causes a corresponding rise in the steam line pressure near the MSIVs as shown in figure 6-22. The steam flow at the reactor vessel and pressure rise in the vessel steam dome are shown in figures 6-23 and 6-24, respectively. The net (void + Doppler + scram) and scram reactivity components are shown in figure 6-25. The maximum positive value of net reactivity was 0.71 and occurred at 2.03 seconds. The power level variation during the event is shown in figure 6-26 with the peak power of 476-percent NBR occurring at 2.22 seconds. The maximum value of core average heat flux was 135.5-percent NBR at 2.59 seconds as shown in figure 6-27.

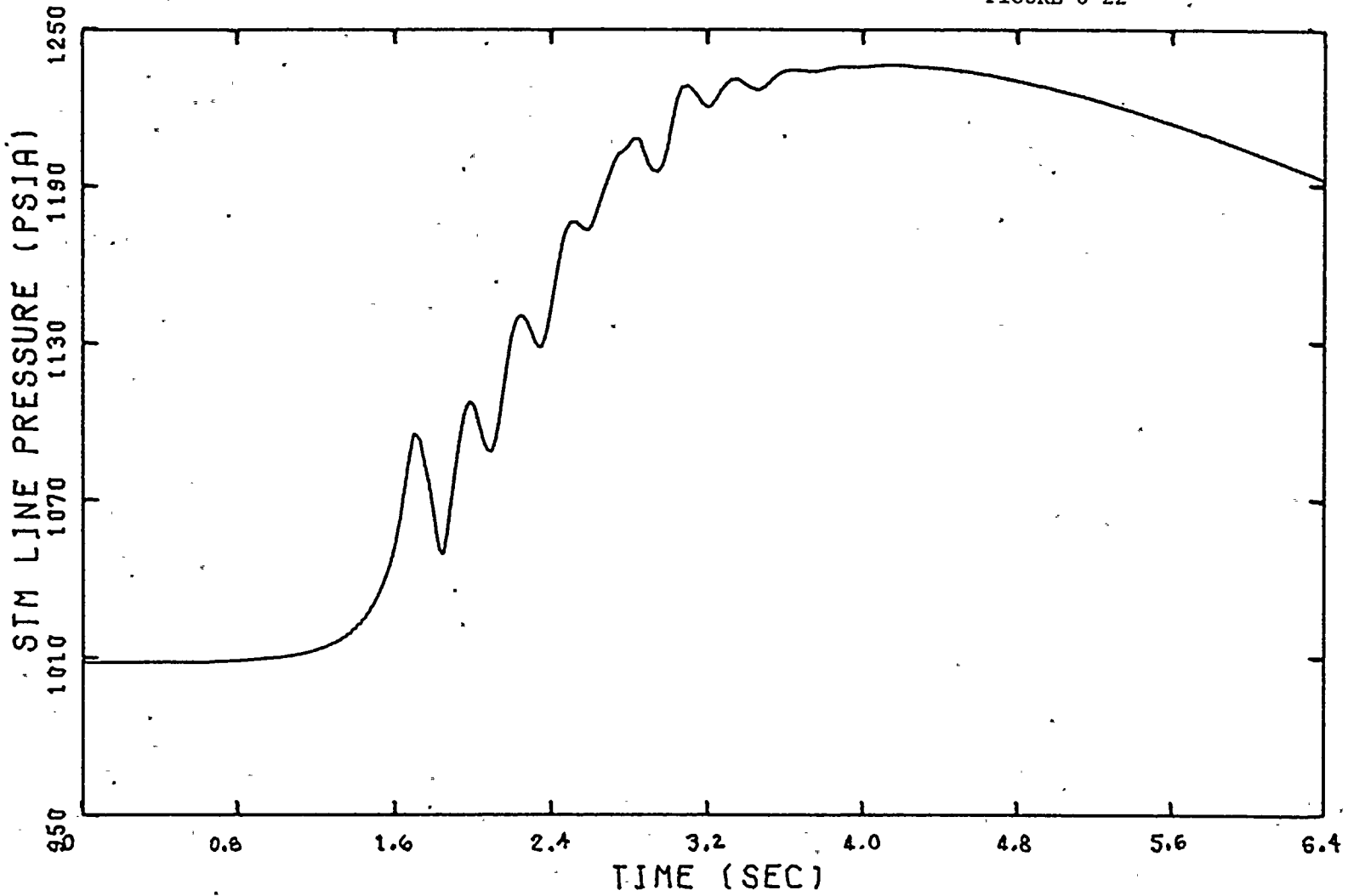
BF3 EOC5 LICENSING BASIS MSIVC

FIGURE 6-21



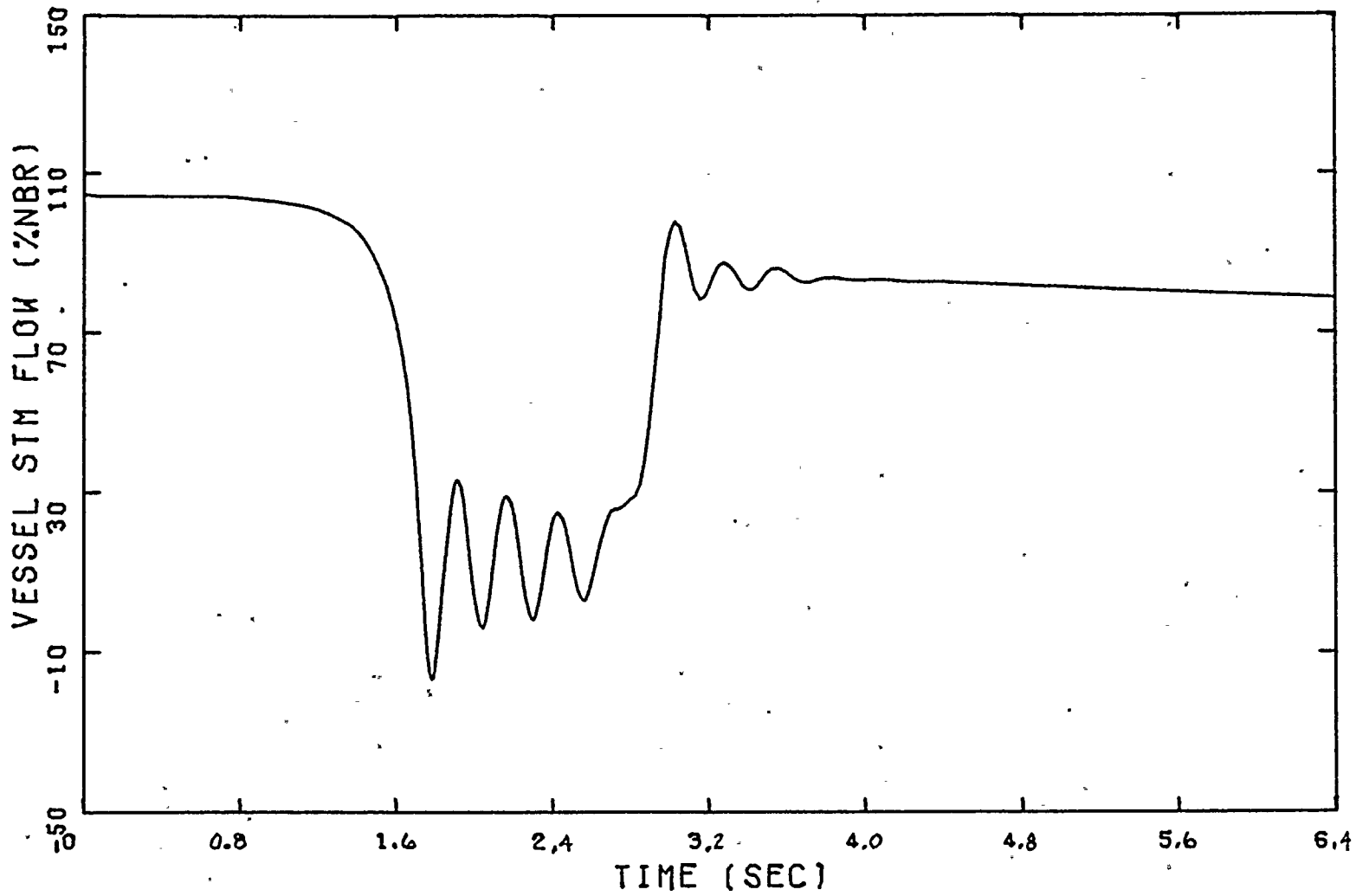
BF3 EOC5 LICENSING BASIS MSIVC

FIGURE 6-22



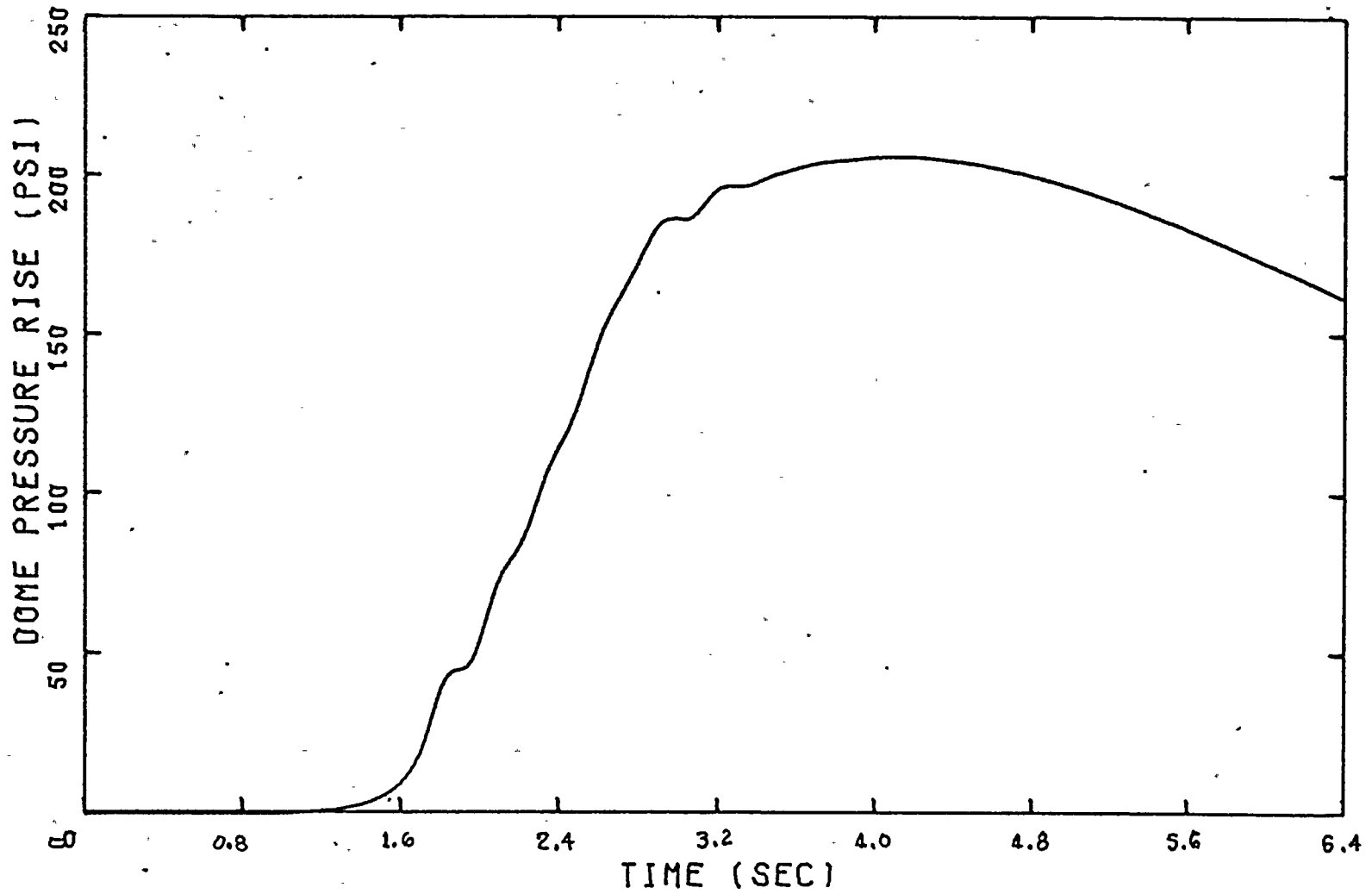
BF3 EOC5 LICENSING BASIS MSIVC

FIGURE 6-23



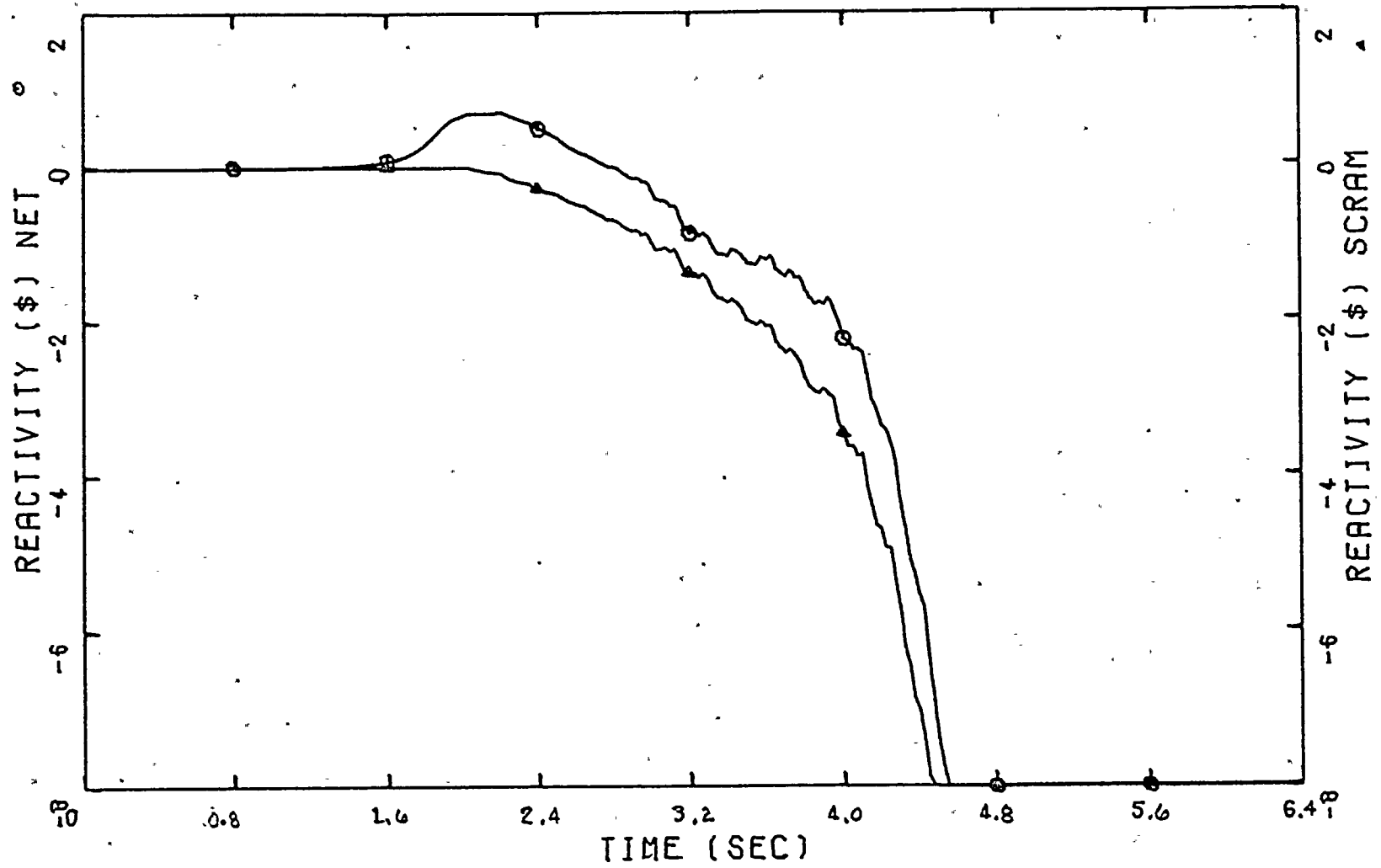
BF3 EOC5 LICENSING BASIS MSIVC

FIGURE 6-24



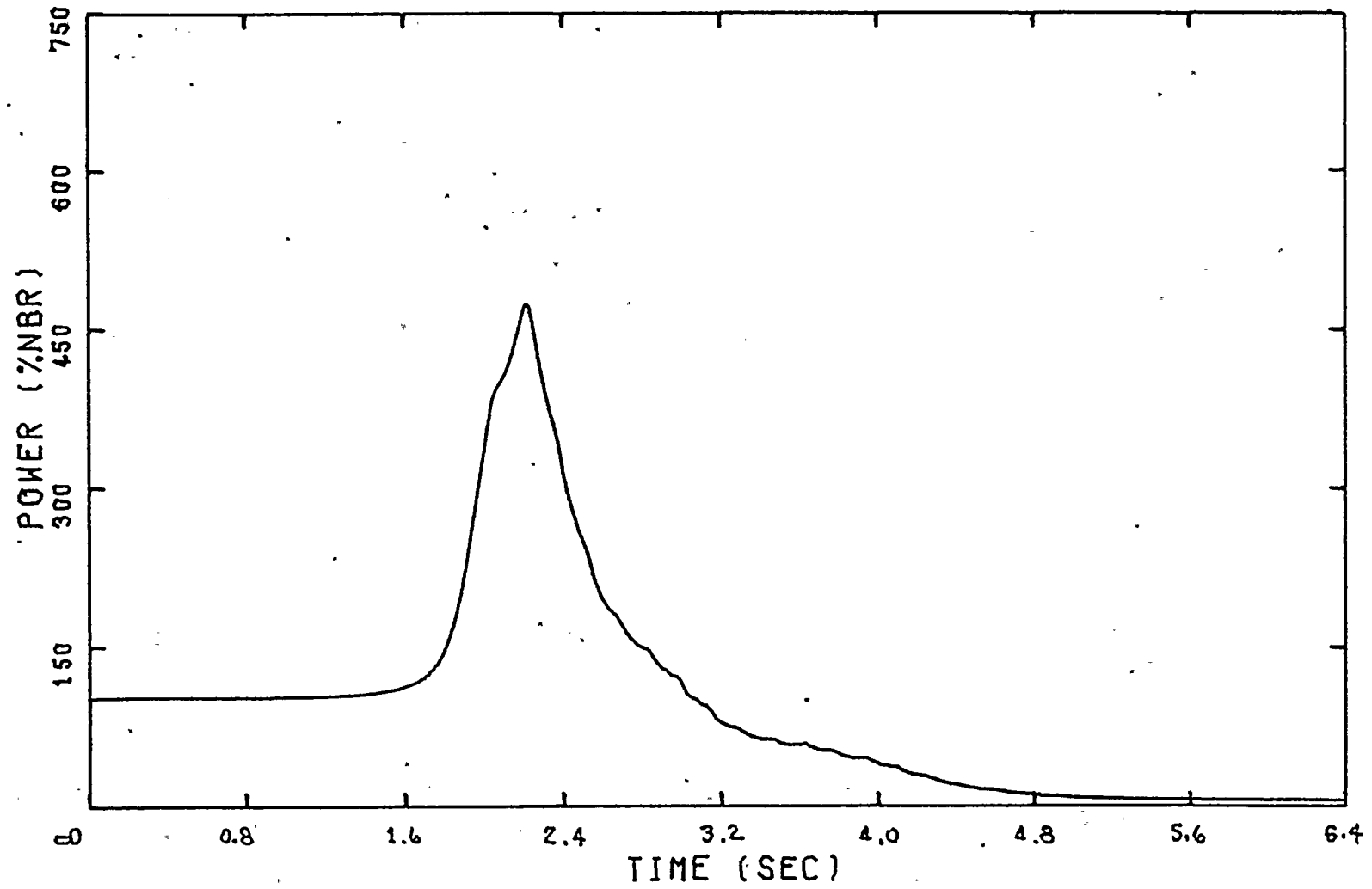
BF3 EOC5 LICENSING BASIS MSIVC

FIGURE 6-25



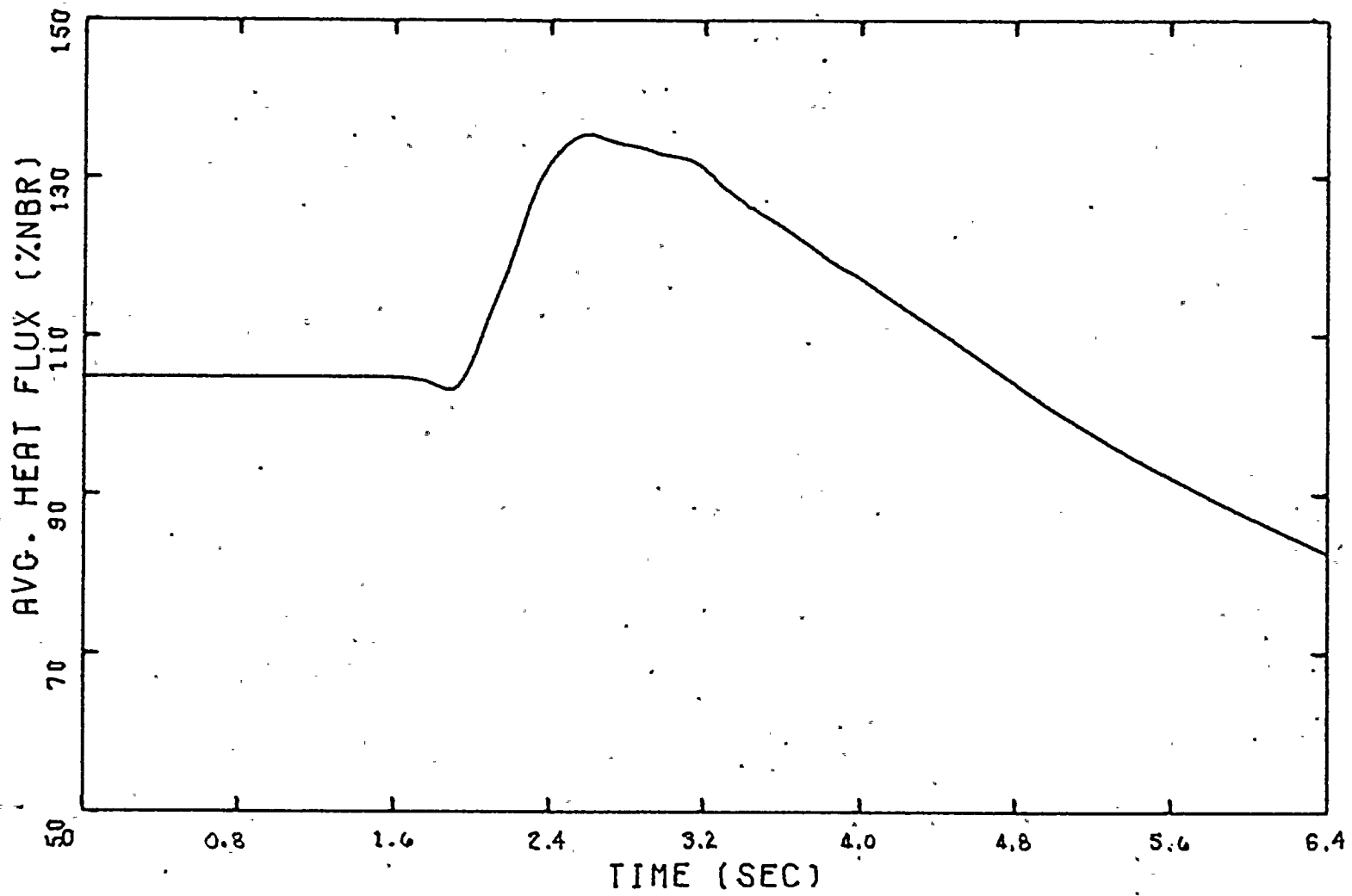
BF3 EOC5 LICENSING BASIS MSIVC

FIGURE 6-26



BF3 EOC5 . LICENSING BASIS MSIVC

FIGURE 6-27



Because the cutoff of steam line flow for the MSIVC event is not as rapid as for fast closure of the turbine control valves, the pressure wave that is excited is not as severe and results in smaller core inlet and exit flow oscillations (figure 6-28) than occurred for the GLRWOB. Because of the much slower coastdown of the pumps for a M-G trip in comparison to opening of the RPT breakers, the overall reduction in core flow rate is not as readily evident for the portion of the event shown in figure 6-28.

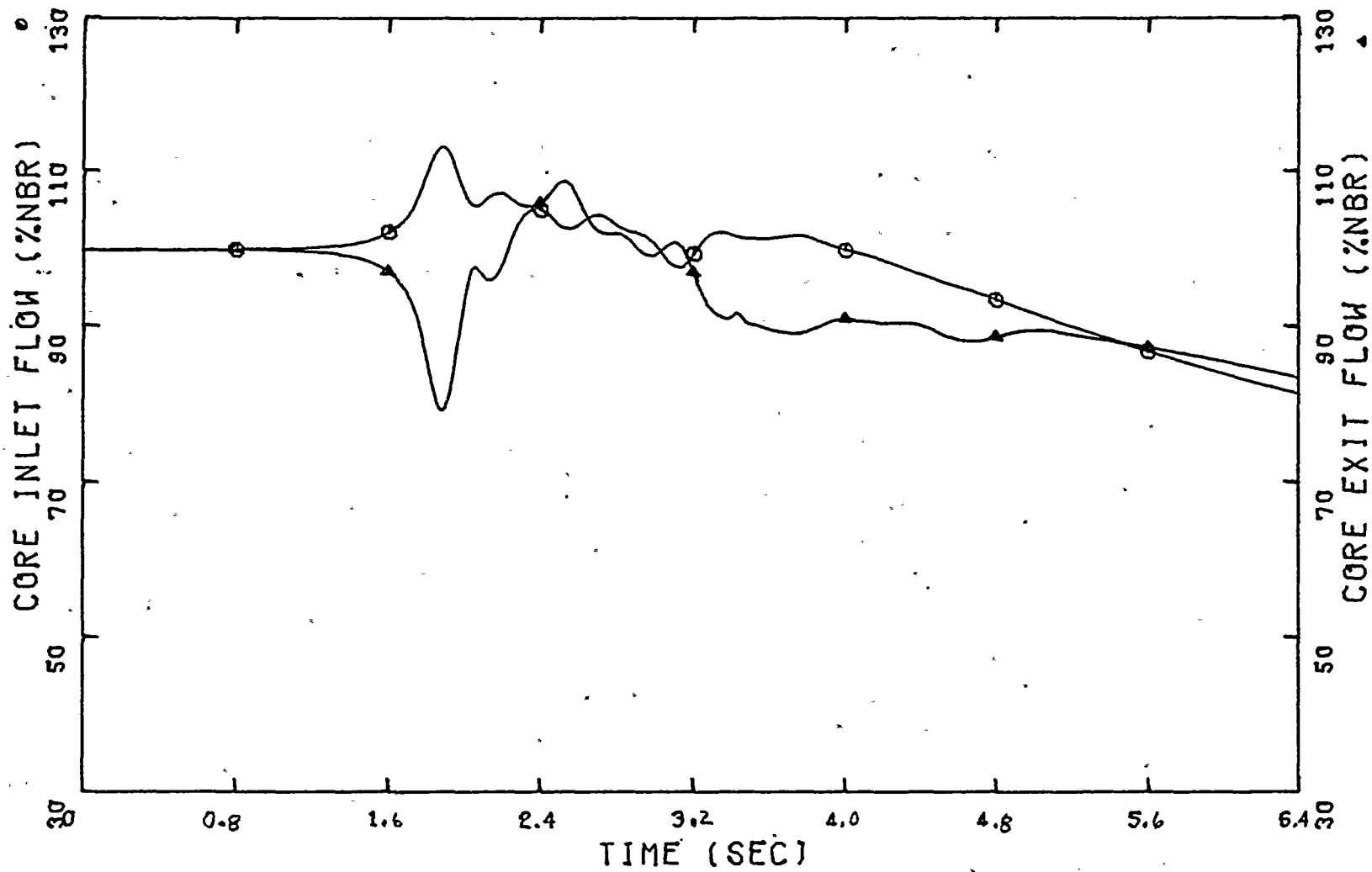
Figure 6-29 shows the behavior of the calculated feedwater flow during the MSIVC event. The reduction in feedwater flow is caused by the reduced feedwater pump output (at approximately constant speed) as the reactor pressure increases. Later in the transient the feedwater flow increases due to both the action of the feedwater controller to increase the pump speed and to the reduction in reactor pressure. The behavior calculated for the narrow range sensed water level is shown in figure 6-30. The initial reduction in water level is primarily due to the collapse of voids inside the core shroud increasing the mass of water in that region and decreasing the level in the vessel downcomer (sensed by NR level instrument). The decrease in level later in the transient is due to the reduction in feedwater flow below the steam flow rate and thus decreasing vessel inventory. Shortly beyond the time scale of figure 6-30, the feedwater flow will increase to a rate higher than the steam flow and recovery of the level will begin. Over a longer period, the feedwater flow will terminate due to loss of extraction steam to drive the feedwater turbines and level will be maintained by the HPCI and RCIC systems.

#### 6.5 Summary of Transient Results

The key transient simulation results for the three limiting pressurization events are summarized in table 6-4. The value of  $\Delta\text{CPR}$  is given for the limiting P8 x 8R bundle for the GLRWOB and FWCF.

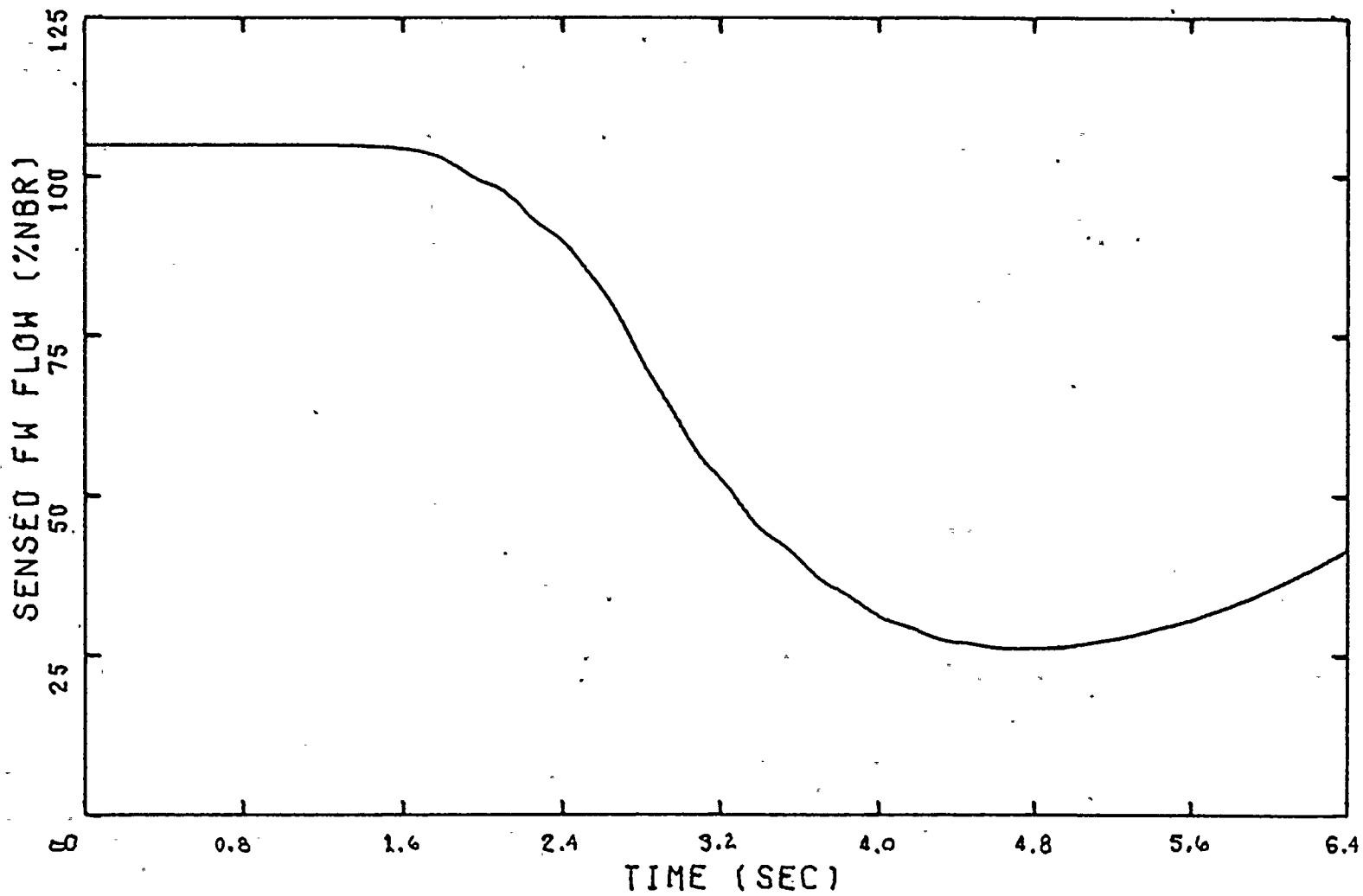
BF3 EOC5 LICENSING BASIS MSIVC

FIGURE 6-28



BF3 EOC5 LICENSING BASIS MSIVC

FIGURE 6-29



BF3 EOC5 LICENSING BASIS MSIVC

FIGURE 6-30

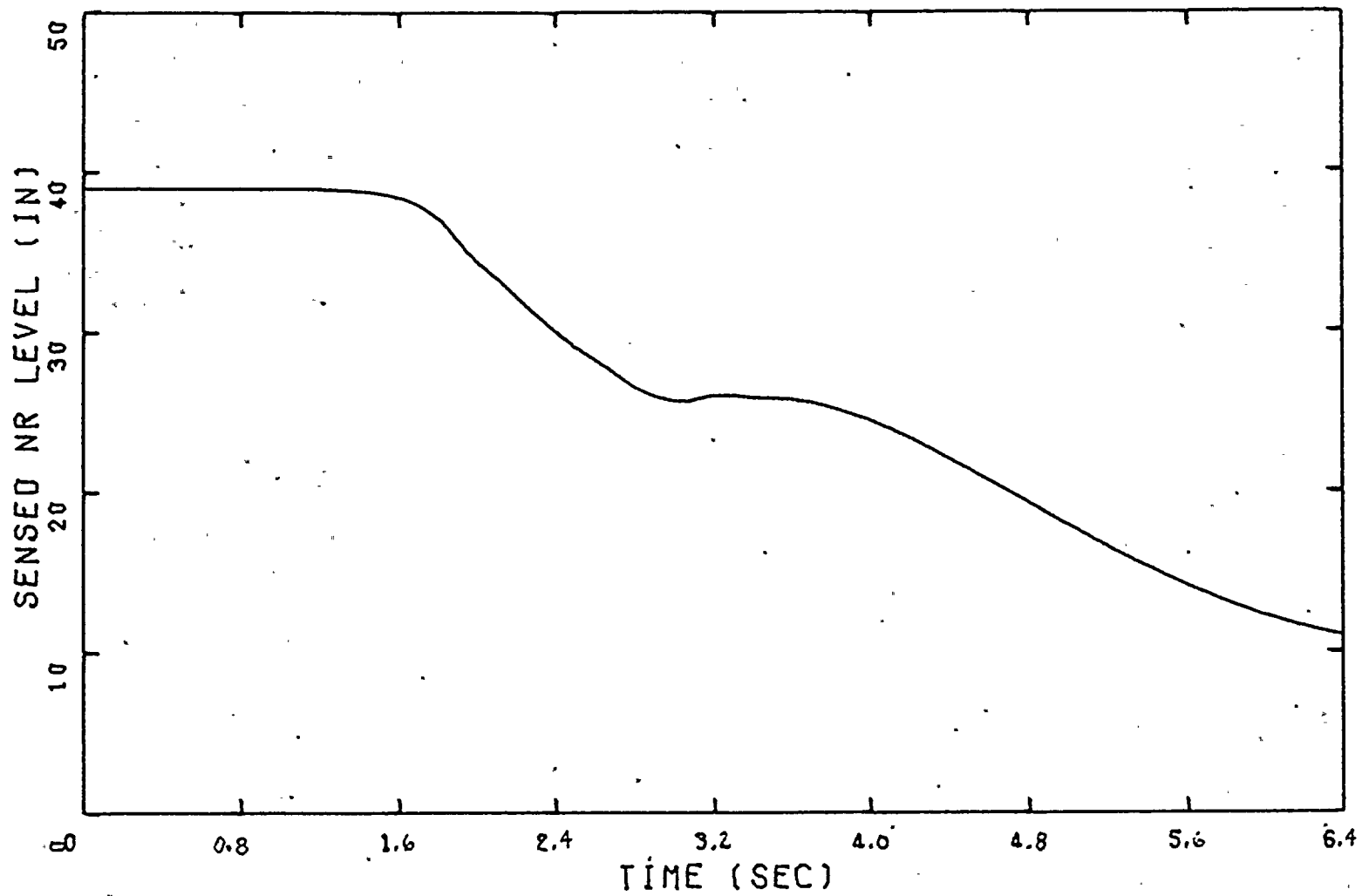


Table 6-4

## Summary of Pressurization Transient Results

<u>Peak value of:</u>	<u>GLRWOB</u>	<u>FWCF</u>	<u>MSIVC</u>
Power (% NBR)	393.	224.	476.
Core avg. heat flux (%NBR)	120.3	114.6	135.3
Steam line pressure (psia)	1212.	1176.	1237.
Vessel pressure (psia)	1234.	1214.	1276.
$\Delta$ CPR	0.22	0.17*	n/a

\*includes 0.03 adder to account for potentially nonconservative initial conditions.

References

- 6-1 "TVA Reload Core Design and Analysis Methodology for the Browns Ferry Nuclear Plant," TVA-EG-047, January 1982.
- 6-2 R. L. Crowther, "Burnup Analysis of Large Boiling Water Reactors," Proceedings of a Panel in Vienna, April 1967 on Fuel Burnup Predictions in Thermal Reactors, IAEA, Vienna (1968).
- 6-3 R. K. Haling, "Operating Strategy for Maintaining An Optimum Power Distribution Throughout Life," TID-7672 (1963).
- 6-4 Browns Ferry Nuclear Plant Technical Specifications, Unit 3, Tennessee Valley Authority.
- 6-5 R. B. Linford, "Analytical Methods of Plant Transient Evaluations for the General Electric Boiling Water Reactor," NEDO-10802, page 2-30, February 1973.
- 6-6 "General Electric Thermal Analysis Basis Data, Correlation, and Design Application," NEDO-10958A, January 1977.
- 6-7 A. F. Ansari, R. R. Gay, and B. J. Gitnick, "FIBWR - A Steady-State Core Flow Distribution Code for Boiling Water Reactors," EPRI NP-1923, July 1981.

## 7. MODEL SENSITIVITY STUDIES

This chapter will present the results of a wide range of sensitivity (model perturbation) studies. The sensitivity studies fall into the general categories below:

- a. Those performed to assess the effect of modeling options and to verify reasonable functioning of models.
- b. Those performed to quantify the effect of model inputs for which the value is uncertain.
- c. Those performed to quantify the effect of uncertainties in actual conditions in the operating plant.
- d. Those performed to quantify conservatism in licensing basis modeling.
- e. Those performed to identify limiting initial conditions for analyses.

The base cases for all sensitivity studies are the licensing basis analyses for Browns Ferry unit 3 at projected end of cycle 5 conditions as presented in chapter 6 and are typical of expected future operating cycles of all three Browns Ferry units.

Sensitivity studies were performed for each of the three limiting pressurization transients but the most extensive set of studies was performed for the GLRWOB event since it is normally most limiting for critical power ratio. Some of the sensitivity studies performed for the GLRWOB were repeated for the FWCF and MSIVC events to verify the applicability of conclusions based on the GLRWOB for these transients. In addition special sensitivity studies were made for the FWCF and MSIVC events for model options or inputs exercised by these transients but not used by the GLRWOB event.

## 7.1 GLRWOB Sensitivity Studies

A summary of the sensitivity studies performed for the GLRWOB event is presented in table 7-1. As discussed earlier, this table includes analyses performed for several different reasons and not all of the perturbations in table 7-1 reflect uncertainties in the licensing basis RETRAN model for Browns Ferry. The table presents the change from the base case in maximum transient reactor power level ( $\Delta Q$ ), maximum core average fuel rod heat flux ( $\Delta q$ ), peak vessel steam dome pressure ( $\Delta P_{VSD}$ ), and the change in the ratio of transient  $\Delta$ CPR over initial CPR ( $\Delta$ RCPR).

### 7.1.1 Nuclear Model

The major uncertainty components related to the reactor core nuclear model are the three reactivity components (void, scram, and Doppler) and the uncertainty in the prompt moderator heating. The uncertainty in each of these components is discussed and the model sensitivity described in the sections below.

#### 7.1.1.1 Void Reactivity

The uncertainty in the void reactivity coefficient inherent in the 1-D kinetics model is composed of four components: (1) uncertainty in the 3-D simulator void model; (2) uncertainty in the dependence of reactivity on water density in the basic lattice physics code; (3) uncertainty in the transformation between 3-D and 1-D water densities and; (4) uncertainty due to inexact fitting of the collapsed 1-D cross section to the polynomial forms used by RETRAN. The first two components reflect the uncertainty in the 3-D simulator calculation (reference 7-1) and the second two components represent the additional uncertainty in the 1-D representation.

## Key Results of Sensitivity Studies for GLRWOB Transient

<u>Description of Modification to Base Model</u>	$\Delta Q$ (% NBR)	$\Delta q$ (% NBR)	$\Delta P_{VSD}$ (psi)	$\Delta RCPB$
<u>Nuclear Model</u>				
Void coefficient 13% more negative	+ 149.9	+ 5.53	+ 4.9	+ 0.030 *
Scram reactivity reduced 10%	+ 23.2	+ 1.33	+ 3.3	+ 0.012 *
Doppler coefficient reduced 10%	+ 6.6	+ 0.40	+ 0.8	+ 0.003 *
Prompt moderator heating reduced 25%	+ 10.0	+ 1.29	+ 1.5	+ 0.007 *
<u>Core Thermal-Hydraulics Modeling</u>				
Fuel pin radial nodes increased 50%	+ 0.5	- 0.22	+ 0.3	+ 0.002
Fuel rod gap conductance increased 25%	- 11.0	+ 1.55	- 1.5	- 0.015
Fuel conductivity reduced 5% and heat capacity increased 5%	+ 9.4	- 0.42	+ 0.4	+ 0.009
Increase core pressure drop by 1.5 psi	+ 4.2	+ 0.39	+ 0.8	+ 0.003 *
Redistribute 5% of core inlet pressure loss to core exit	+ 1.5	+ 0.13	+ 0.3	+ 0.002 *
Increase active core nodes to 24	- 1.7	- 0.08	+ 0.1	+ 0.004 *
Reduce initial core bypass flow by 20%	+ 1.1	+ 0.13	+ 0.1	+ 0.002 *
Eliminate core bypass flow junction 109	- 63.5	- 3.01	- 2.7	- 0.015
Detailed noding of fuel channel conductor	- 24.5	- 1.61	- 2.0	- 0.013
Use HEM in thermal-hydraulics solution	- 115.3	- 0.30	+ 4.4	+ 0.009 *
Reduce subcooled voids by 30%	+ 66.6	+ 2.24	+ 2.0	+ 0.012 *
<u>Recirculation System Model</u>				
Reduce recirc pump head 10%	+ 5.8	+ 0.31	+ 0.3	+ 0.002 *
Double recirc loop fluid inertia	+ 9.8	+ 0.68	+ 0.9	+ 0.005 *
Double jet pump fluid inertia	- 60.9	- 2.10	- 0.6	+ 0.005 *
Jet pump M ratio increased 7 %	+ 48.0	+ 2.30	+ 2.3	+ 0.011 *
Jet pump N ratio increased 10%	- 0.5	- 0.03	0.0	0.000
Jet pump head increased 10%	+ 6.8	+ 0.35	+ 0.3	+ 0.002 *
No carryunder from separators	- 3.9	- 0.16	- 0.4	0.000
Initial separator liquid inventory reduced 25%	+ 0.7	+ 0.03	- 0.2	0.000
Double inertia on separator junction 141	+ 5.8	+ 0.24	+ 0.2	+ 0.001 *
Best estimate separator inertia modeling	- 95.4	- 2.48	- 0.3	- 0.002
Reduced separator pressure drop by 0.5 psi	- 2.8	- 0.27	- 0.4	- 0.001
Equilibrium separator model	- 15.7	- 0.66	- 1.3	- 0.004

Table 7-1 (Continued)

## Key Results of Sensitivity Studies for GLRWOB Transient

<u>Description of Modification to Base Model</u>	$\Delta Q$ (% NBR)	$\Delta q$ (% NBR)	$\Delta P_{VSD}$ (psia)	$\Delta RCPR$
<u>Vessel &amp; Steam Line Nodes</u>				
Increase Inertia of volumes 100, 180, & 190 by 20%	- 1.7	- 0.05	+ 0.1	+ 0.001 *
Decrease steam dome volume by 5%	+ 21.9	+ 0.97	+ 3.2	+ 0.007 *
Decrease upper downcomer volume by 5%	+ 3.6	+ 0.15	+ 0.6	+ 0.001 *
Reduce steam line volume by 5%	+ 10.8	+ 0.20	+ 0.5	+ 0.002 *
Reduce steam line flow area by 5%	+ 2.8	+ 0.12	0.0	+ 0.001 *
Increase steam line inertia by 7%	+ 14.8	+ 1.11	+ 0.8	+ 0.009 *
Reduce steam line pressure drop by 10%	+ 19.3	+ 0.82	+ 0.5	+ 0.005 *
Nominal relief valve modeling (capacity, setpoints, & delay)	0.0	0.00	- 36.9	+ 0.017
Increase steam line nodes to 11	- 4.2	- 0.39	- 0.7	- 0.003
<u>Miscellaneous</u>				
Nominal scram solenoid delay	- 20.8	- 0.78	- 1.0	- 0.005
Nominal fast TCV closure time	- 50.9	- 2.05	- 2.3	- 0.012
Nominal RPT delay	- 17.0	- 0.94	- 1.0	- 0.005
Nominal pump coastdown constant	- 6.9	- 0.46	+ 0.3	- 0.003
Initialized for 100%-NBR steam flow	- 48.7	- 7.15	- 11.9	- 0.006
Nominal measured scram speed	- 99.7	- 5.28	- 14.6	- 0.055
Final feedwater enthalpy reduced 20 Btu/lb	- 14.0	+ 1.93	0.0	- 0.012
Initiated on load line at reduced flow (approx. 71% rated)	- 209.6	- 30.78	- 32.1	- 0.006

$\Delta Q$  = perturbed case peak power (% NBR) minus base case value

$\Delta q$  = perturbed case peak core average heat flux (% NBR) minus base case value

$\Delta P_{VSD}$  = perturbed case peak vessel dome pressure (psia) minus base case value

$\Delta RCPR$  = perturbed case  $\Delta CPR/ICPR$  minus base case value

\* Indicates items included in determination of uncertainty in model RCPR

Comparison of the 3-D simulator to measured plant data as presented in reference 7-2 is useful in assuring that no gross bias in the 3-D simulator's void reactivity calculation exists. However, such comparisons do not readily allow accurate quantification of the uncertainty. Adequate measured data is not available to allow rigorous determination of the 3-D code's uncertainty therefore an estimate of the possible uncertainty was developed by examining the analytic models.

The voids in the 3-D simulator are calculated using the empirical CISE slip correlation (reference 7-3). The empirical parameters in the CISE correlation were developed to minimize the differences in model calculations and experimental data for a wide range of conditions. The standard deviation of the differences between measured void fractions and model calculations was 11 percent. To determine the uncertainty in the CISE model for void coefficients, revised empirical parameters were developed which maximized the void change for increases in pressure while maintaining a standard deviation of less than 11 percent in void fraction from the original model for the range of data used in developing the correlation. Utilizing the Browns Ferry unit 3 EOC5 core and transient model initial conditions, the reactivity change associated with a pressure increase of 75 psi was evaluated with the 3-D simulator for the original CISE correlation parameters and those for maximum pressure coefficient. These analyses indicated a difference of 5.3 percent in void reactivity which is a measure of the uncertainty in the 3-D simulator void model.

The variation in nodal  $k_{\infty}$  for instantaneous changes in void in the 3-D simulator is based on tables computed by the TVA LATTICE program (reference 7-4). To estimate the uncertainty in void reactivity due to uncertainties in the calculation of the change in  $k_{\infty}$  with void,  $[k(v)/k(40)]$ , computed by LATTICE, calculations were performed with the KENO Monte Carlo neutron

transport program (reference 7-5). The variation in nodal reactivity with void changes was computed with KENO and the difference in  $k(v)/k(40)$  between LATTICE and KENO was developed for three fuel bundles. The effect of these differences on void reactivity was evaluated by applying the correction to each node in the 3-D simulator and evaluating the effect on reactivity for a 75 psi pressure increase. These analyses indicated an uncertainty of approximately 8.2 percent in void reactivity based on the differences between LATTICE and KENO for infinite lattice physics calculations. The total 3-D simulation void reactivity uncertainty (CISE model and lattice physics data) was estimated to be 9.8 percent.

The uncertainty in the water density transformation between the 3-D and 1-D codes is basically due to the uncertainty in the manner the water density perturbation from transient initial conditions is distributed in the radial plane. Table 2-7 yields an estimate of 6-percent uncertainty in reactivity due to uncertainties in the radial distribution of water density perturbations.

The uncertainties due to errors in fitting 1-D cross sections cannot be completely separated from the uncertainty in 3-D to 1-D water density transformation since these also result in fitting errors. Based on a range of cross section files developed for use with RETRAN, the combined reactivity uncertainty due to transformation and fitting errors is estimated to be less than 8.5 percent. Combining the 1-D uncertainty (8.5 percent) with the uncertainty in the 3-D simulator void reactivity (9.8 percent) results in a total of 13-percent uncertainty in the void reactivity in the 1-D model.

The base case RETRAN cross section file was modified to obtain approximately a 13-percent increase (more negative) in void coefficient of reactivity. Utilizing the modified cross sections the GLRWOB transient was

rerun to obtain the sensitivity results for void reactivity shown in table 7-1. The peak power and heat flux are greatly increased for the increased void coefficient case due to the relative closeness to prompt criticality. A moderate increase of 4.9 psi in peak vessel dome pressure occurred. The 13-percent void coefficient change resulted in a 0.030 increase in RCPR which is the largest component in the model uncertainty.

#### 7.1.1.2 Scram Reactivity

Comparisons were made between LATTICE and KENO of the infinite lattice control strength (change in  $k_{\infty}$  for control rod inserted to control rod withdrawn configurations). The comparisons were made for several bundle designs and inchannel void fractions. The differences in control strength ranged between 0.5 and 4.8 percent. These comparisons confirm that an uncertainty in scram reactivity of 10 percent due to lattice physics uncertainties is a conservative estimate. As noted in section 6.1.3 there are several conservative assumptions employed in the 1-D representation of scram reactivity which tend to offset any potential nonconservatisms in the lattice physics data.

The scram speeds were adjusted in the RETRAN model to achieve a 10 percent reduction in scram reactivity during the pertinent part of the GLRWOB transient (i.e., before peak heat flux is reached). The results of the RETRAN analysis indicate a moderate increase in peak power, heat flux, dome pressure, and RCPR for the 10-percent decrease in scram reactivity.

#### 7.1.1.3 Doppler Reactivity

The Doppler reactivity calculations by TVA's LATTICE program were compared to Hellstrand's experimental resonance integral data for U-238 (references 7-6 and 7-7). A normalization factor of 1.12 (applied in the 3-D simulator) was found to give excellent agreement between LATTICE and

the Hellstrand data. The uncertainty in the Doppler reactivity was determined by examining the quoted uncertainties in the Hellstrand correlation parameters ( $\lambda_0$  and  $\beta$ ) which are estimated to contribute 9-percent uncertainty to the Doppler reactivity. The uncertainty in the calculation of the average increase in fuel pin temperature during a pressurization transient was estimated to be less than 4 percent yielding a combined Doppler reactivity uncertainty of 10 percent.

The base case RETRAN cross section file was modified to obtain a 10-percent reduction in the Doppler coefficient of reactivity. The modified cross section file was then utilized to perform the GLRWOB analysis. As shown by the results in table 7-1, a 10-percent reduction in Doppler coefficient produces a slightly more severe transient but its effect is small relative to the void and scram reactivity uncertainties.

#### 7.1.1.4 Prompt Moderator Heating

In the RETRAN model for Browns Ferry, the fraction of power deposited directly in the moderator decreases approximately linearly with water density. For the water density distribution initially present for the base case the core average fraction of power deposited promptly in the moderator was 0.019. Based on reference 7-8, the uncertainty in the prompt heating was assumed to be 25 percent and this reduction was made uniformly as a function of water density. The RETRAN calculations with a 25-percent reduction in prompt heating yielded increases of 10-percent NBR in peak power, 1.3-percent NBR in peak heat flux, 1.5 psi in peak dome pressure, and 0.007 in RCPR.

#### 7.1.2 Core Thermal-Hydraulics Modeling

A range of core thermal-hydraulic modeling sensitivities was investigated including nodalization, irreversible pressure loss magnitude

and distribution, core bypass flow modeling and magnitude, effect of slip and subcooled voids, fuel channel conductor modeling, and fuel pin modeling and properties.

#### 7.1.2.1 Fuel Pin Modeling

A 50-percent increase in radial nodalization (from 10 to 15 nodes in pellet and from 4 to 6 in clad) was made in the fuel rod conductors to verify that the base model noding is adequate. Only very minor differences from the base model were observed for the increased noding indicating that the base case noding is adequate.

The core-average fuel rod gap conductance used in the licensing basis model is set conservatively low and is specified as uniform axially and constant during the transient which further increases the conservatism. To assess the amount of conservatism in the gap conductance modeling, a run was made with gap conductance increased. It was estimated that a 25-percent increase would be approximately equivalent to a best-estimate value and the effects of the expected axial and time variation in gap conductance. Best-estimate gap conductance modeling was found to decrease the peak power by 11-percent NBR, increase peak core average heat flux by 1.55-percent NBR, decrease peak dome pressure by 1.5 psi and reduce RCPR by 0.015. Thus the licensing basis modeling of gap conductance yields a significant conservative bias in thermal limits.

The uncertainties in  $UO_2$  and Zircaloy properties (conductivity and specific heat) were estimated to be approximately 5 percent. The properties as a function of temperature were changed 5 percent each in the direction required to increase the fuel rod time constant (reduced conductivity and increased heat capacity). As shown in table 7-1, the change in transient results with the modified fuel properties is less than

the estimated conservative bias in fuel rod gap conductance modeling. Therefore the overall licensing basis fuel rod model has a conservative bias and no additional uncertainty penalty is appropriate.

#### 7.1.2.2 Core Pressure Drop

The uncertainty in the core pressure drop is estimated to be less than 1.5 psi at design conditions. Increasing the core pressure drop by 1.5 psi resulted in small increases (slightly more severe) in all quantities. It should be noted that changes in core pressure drop cannot be made without a corresponding change in the driving head. In this study the core pressure drop decrease was balanced by reducing the frictional pressure losses in the jet pump diffuser. Alternate approaches would be to modify the head produced by the recirculation system. However, the uncertainties in pump head and operating point are considered separately in this study.

The distribution of pressure losses between core inlet, internal, and exit areas for the Browns Ferry RETRAN model was developed to provide agreement with a program which performs detailed core thermal-hydraulic calculations based on empirical models verified against measured data. To assess the effect of uncertainties in the distribution of the pressure losses, the core inlet pressure loss was reduced 5 percent with a corresponding increase in the core exit loss. The redistribution of pressure losses between core inlet and exit produced a slightly more severe result for the GLRWOB event (RCPR increased 0.002).

#### 7.1.2.3 Core and Core Bypass Modeling

The adequacy of using twelve active core volumes and fuel rod conductors to provide water density and fuel temperature feedback to the

nuclear model was assessed by subdividing the nodding to obtain 24 active sections. The change in GLRWOB transient key results were small for the increased nodding indicating that the base model core nodding is adequate.

The uncertainty in the initial core bypass flow fraction was conservatively estimated to be less than 20 percent. The initial bypass flow was reduced by 20 percent which resulted in a slightly more severe transient but the overall effect was small.

The base model utilizes two bypass paths. One path (junction 101) is between the vessel lower plenum and core bypass volume such that the flow is proportional to the pressure difference across the core support plate. The second path (junction 109) is between the unheated core inlet section and the bypass volume such that the flow is proportional to the fuel channel wall pressure differential. The effect of the bypass junction 109 on the system response was evaluated by initializing a deck with junction 109 removed and the flow at junction 101 increased to maintain the initial bypass flow fraction. Utilizing this deck for the GLRWOB transient showed that removal of junction 109 significantly reduced the severity of the event. The reason for the sensitivity was traced to differences in the active core inlet flow (junction 1). The flow through junction 109 rapidly decreases during the initial pressurization forcing the active core inlet flow higher than occurs if junction 109 is removed. The higher active core inlet flow augments the void collapse caused by the pressure increase further increasing the positive void reactivity insertion and producing a more severe transient than occurs without junction 109. A portion of the bypass flow in the operating reactor is dependent upon the fuel channel wall pressure differential; however, the amount varies significantly from bundle to bundle depending upon the bundle power. An average power channel pressure differential as used in the RETRAN model overestimates the

reduction in bypass flow fraction for a pressure increase relative to that which would be obtained from a multi-channel model with a distribution of bundle powers. Therefore, part of the difference observed when junction 109 is removed represents a conservative bias in the RETRAN model.

A single lumped conductor (912) represents the fuel channels of all 764 bundles in the core preserving the total surface area, channel volume, and thickness. Conductor 912 is bounded by the lumped bypass volume on one side and a mid-core volume (12) on the other. During a pressure increase the thermal equilibrium assumption in RETRAN-02 causes the coolant temperature to increase resulting in heat being transferred into conductor 912 and stored. Since this heat is not available to produce voids the severity of the power rise is increased. To examine the effect of the simplified fuel channel conductor modeling, a deck was created with the core bypass volume subdivided into an axial stack of 12 volumes with 12 channel wall conductors each associated with a bypass volume on one side and the corresponding active core volume on the other side. The results of the GLRWOB transient with the more detailed fuel channel conductor modeling were significantly less severe than the base model results. In fact the detailed conductor model results were comparable to those obtained by eliminating conductor 912 from the base model. Thus the simplified fuel channel conductor modeling introduces a conservative bias into the licensing basis model.

#### 7.1.2.4 Void Models

The RETRAN "Algebraic Slip" option is employed in the TVA model. This option is a drift flux model developed by EPRI (reference 7-9). To assess the effects of uncertainties in drift flux parameters on transient results an analysis was performed without slip between the liquid and vapor phases

using the RETRAN homogeneous equilibrium model (HEM) as a bounding assumption. The HEM assumption was also used in making the transformation between 3-D and 1-D model water densities for producing the 1-D cross section file. The results of the GLRWOB event utilizing the HEM assumption resulted in a much lower (115-percent NBR) peak power but no significant change in peak heat flux. The peak dome pressure increased 4.4 psi and RCPR was increased by 0.009, representing one of the larger model uncertainties.

Since RETRAN-02 assumes thermal equilibrium between the vapor and liquid phases (except in special separated volumes utilizing a nonequilibrium model), subcooled voids are not directly treated. However, a profile fit subcooled void model developed by EPRI (reference 7-10) is used to determine the water densities for evaluating the 1-D cross sections. The effects of uncertainties in the subcooled void model were evaluated by performing an analysis without the profile fit model (i.e., densities were taken directly from RETRAN's thermal-hydraulic solution for evaluating the cross sections). Since the uncertainty in subcooled voids is estimated to be less than 30 percent the resulting changes from the base case were decreased by multiplying by a 0.3 factor. The 30-percent reduction in subcooled voids significantly increases all the key quantities listed in table 7-1.

### 7.1.3 Recirculation System Model

Uncertainties in operating conditions associated with the recirculation pump, loop piping, jet pumps, and steam separators were estimated. The effects of the uncertainties and some modeling assumptions on the GLRWOB event were evaluated with sensitivity studies.

#### 7.1.3.1 Recirculation Loop

The pressure head produced by the recirculation pump operating at licensing basis conditions was reduced by 10 percent. A compensating reduction in the recirculation loop frictional pressure loss was made so that the jet pump operating point was not changed. The reduction in recirculation pump head caused each of the four key quantities in table 7-1 to be slightly more severe.

To account for the uncertainty in the effective fluid inertia in the recirculation loop the inertia for volumes 200, 220, and 240 was doubled and the associated junction inertias determined. Doubling the recirculation loop fluid inertias produced a moderate increase in transient severity.

#### 7.1.3.2 Jet Pump Model

The sensitivity of model results to uncertainties in the effective fluid inertia associated with the jet pumps was established by doubling the base case value of jet pump inertia. The increased inertia caused a 60.9-percent NBR decrease in peak power, 2.1-percent NBR decrease in peak core average heat flux, a 0.9 psi increase in peak dome pressure, and an increase of 0.005 in RCPR. The reduced peak power and heat flux are caused by a reduction in the maximum core inlet flow during the initial pressurization. The decreased inlet flow also offsets the decreased heat flux and increases the value of RCPR.

The effects of uncertainties in the initial operating point of the jet pumps were evaluated by increasing (separately) the initial M ratio by 7 percent, the initial N ratio by 10 percent, and the jet pump head by 10 percent. These changes were accomplished by changing the irreversible pressure loss coefficients at junctions 181, 240, and 260. The increase in

M ratio produced moderately more severe results for all of the key quantities. Increasing the jet pump head produced only slightly more severe results while the N ratio change had no appreciable effect.

#### 7.1.3.3 Steam Separator Model

The effect of the steam carryunder fraction from the separators (0.2 percent in base model) was examined by decreasing the core inlet enthalpy to allow initialization for zero carryunder. Initialization for zero steam carryunder was a minor perturbation and did not significantly affect any key result. A similarly insignificant change occurred when the initial liquid inventory in the steam separators was decreased by 25 percent.

In the licensing basis model the fluid inertia for the liquid exit path (junction 141) was changed to the value obtained by dividing the separator height by the cross sectional flow area. When the inertia of junction 141 is doubled only slight increases in peak power and RCPR are observed. As described in section 6.1.5 the effective fluid inertia of the steam separators from vendor test data is applied at the separator inlet junction (125) in the licensing basis model. In the "best estimate" modeling used for comparison to measured transient data in chapters 3 and 4 the test data separator inertia was divided between junctions 125 and 141. The conservatism in the licensing basis modeling was assessed by comparing the base case to the results with the inertia divided equally between the separator inlet and exit. The best estimate separator inertia modeling produced large reductions in peak power (95-percent NBR) and heat flux (2.5-percent NBR) but only small reductions in peak pressure (0.3 psi) and RCPR (0.002).

The pressure drop across the steam separator in the TVA RETRAN model is initialized to a value determined by the inlet quality and flow rate using an equation developed from manufacturer's teststand results and shown to yield conservatively high values. The sensitivity of GLRWOB transient results to the separator pressure drop was assessed by decreasing the value in the base model by 0.5 psi. The 0.5 psi reduction in separator pressure drop slightly reduced the severity of the event.

The Browns Ferry model utilizes the RETRAN separator model with the state property solution which does not assume thermal equilibrium between the vapor and liquid phases ("nonequilibrium separator" model). RETRAN-02 also has available an equilibrium separator model which does assume thermal equilibrium in the state property solution. The magnitude of the nonequilibrium effects in the separator was tested by running a GLRWOB transient utilizing the equilibrium separator model. Use of the equilibrium separator reduced the severity of the transient as expected.

#### 7.1.4 Vessel and Steam Line Nodes

The sections below present the sensitivity studies performed on the vessel nodes (primarily in the dome and downcomer) and main steam line representations. Most of the sensitivity studies relate to uncertainties in geometric data (volumes, areas, and inertias). Since "as built" drawings were employed in geometric data calculations the uncertainties are small. One contributor to the geometric data uncertainty is due to the need to base areas on the "stream tube" area in one-dimensional thermal-hydraulic codes such as RETRAN.

##### 7.1.4.1 Vessel Nodes

The fluid inertia for vessel downcomer and lower plenum volumes (100, 180, and 190) is low due to the large flow area in relation to flow length.

The inertia of these volumes is not expected to significantly affect the transient results and this was confirmed by increasing the inertia by 20 percent for these volumes. The uncertainty in the base model volume for the vessel steam dome (170) and upper downcomer (160) was estimated to be 5 percent. Decreasing these volumes by 5 percent produced more severe transient results for the GLRWOB as expected. The effect of the reduction for volume 160 was slight but a 5-percent reduction for volume 170 produced significant increases in peak power and RCPR.

#### 7.1.4.2 Steam Line Model

Uncertainties in steam line geometric data were investigated by uniformly reducing the available fluid volume and flow area in the steam line by 5 percent. Each of the reductions caused slightly more severe results for the GLRWOB. A uniform 7-percent increase in the steam line fluid inertia caused modest increases in peak power, heat flux, and pressure but resulted in a substantial (0.009) increase in RCPR. The increased steam line inertia causes a longer period and higher amplitude pressure wave in the steam line. This has the effect of delaying the core pressurization but making it faster and more severe.

The steam line form loss coefficients in the Browns Ferry RETRAN model were developed to provide a pressure drop between the vessel steam dome (170) and last steam line volume (340) which provides good agreement with measured data. The comparisons to pump trip transients presented in chapter 3 indicate that excellent agreement is obtained and indicate a uncertainty of less than 10 percent. The steam line loss coefficients were changed uniformly to lower the pressure drop by 10 percent and the GLRWOB transient was reanalyzed. The lower steam line pressure drop results in a

slightly greater pressurization rate in the core and produces more severe transient results as shown in table 7-1.

In the licensing basis model, the relief valve opening delay and stroke time are specified at maximum specification values (slower than expected). Also the capacity is set in compliance with the ASME rating which is less than the expected values, and the setpoints are increased by 1 percent over their nominal values to account for calibration uncertainty and drift. The licensing basis modeling of relief valves produces a conservatively high estimate of peak vessel pressure. However, when the RETRAN model was utilized with nominal modeling of the relief valves the calculated value of RCPR increased for the GLRWOB event. The primary cause of the increase in RCPR was traced to the earlier opening of the relief valves. When the relief valve initially opens there is a momentary increase in the local flow rate near the exit of the core. This acceleration lasts for only a few tenths of a second but tends to decrease the CPR value. The nominal relief valve modeling causes this temporary decrease in CPR to reinforce the minimum CPR calculated due to longer term heat flux and core flow trends. Because of the brevity of the CPR decrease caused by the initial relief valve opening, it would not be associated with any fuel damage even if incipient boiling transition is calculated with a steady-state correlation. Since several conservative biases in the licensing basis model have been identified which combined are of substantially greater magnitude than the relief valve opening effect, no penalty or additional uncertainty to the licensing basis results is warranted.

The main steam lines for the Browns Ferry units are approximately 260 feet long between the vessel and stop/control valves. In the model the

steam lines are divided into six volumes. In order to determine if the base model noding of the steam line is adequate, a model with 11 approximately equal length volumes was developed. The results of the GLRWOB transient with the 11-node steam line were slightly less severe than the base model but no significant differences were observed.

#### 7.1.5 Miscellaneous Sensitivity Results

Several sensitivity runs were performed to assess the degree of conservatism in licensing basis inputs for scram solenoid delay, turbine control valve closure time, recirculation pump trip delay, and recirculation pump coastdown rate. The conservatism due to the rapid closure of the control valve relative to the expected rate is substantial and the combined conservatism in RCPR of these quantities alone is approximately 0.014. The amount of conservatism in the use of 105-percent NBR steam flow instead of the nominal 100 percent was evaluated in addition to the difference between using nominal measured scram speeds and technical specification conformance limit speeds.

The licensing basis deck is initialized for the maximum capability final feedwater enthalpy. To demonstrate the conservatism in utilizing the maximum feedwater enthalpy a deck was initialized for 105-percent NBR steam flow but with the feedwater enthalpy reduced. The sensitivity results in table 7-1 are for a reduction in enthalpy of 20 Btu/lb which is sufficient to account for uncertainties in the feedwater enthalpy and the effect of operation with a feedwater heater steam extraction line valved out. As expected the reduced feedwater enthalpy results in a milder transient demonstrating the conservatism in using the maximum feedwater enthalpy for the GLRWOB transient.

The effect of operation at reduced core power and flow on the GLRWOB transient was investigated by initiating the event from initial conditions determined by reducing the recirculation pumps speed to obtain a load line point at approximately 71-percent core flow. All key GLRWOB transient results were less severe for the load line reduced power and flow case as indicated in table 7-1.

## 7.2 FWCF Sensitivity Studies

A summary of the sensitivity studies performed for the FWCF to maximum demand event is presented in table 7-2. The list of studies presented for the FWCF is not as extensive as for the GLRWOB event since the effect of most of the perturbations for the GLRWOB can be conservatively applied for the FWCF. A representative set of perturbed case results is presented for the FWCF transient and the perturbations were made in the same manner as described for the GLRWOB event. Additional studies were performed on the FWCF transient for models and input which uniquely affect the FWCF.

### 7.2.1 Nuclear Model

As for the GLRWOB transient, the major uncertainty contributions result from the assumed 13-percent uncertainty in void coefficient and 10-percent uncertainty in scram reactivity. Due to the less severe pressurization for the FWCF event, the sensitivity of the key results is approximately one-half as large as obtained for the GLRWOB. The FWCF transient results were found to be insensitive to the 25-percent reduction in prompt moderator heating.

### 7.2.2 Core Thermal-Hydraulics Modeling

The lower power increase for the FWCF event lessened the sensitivity to fuel rod gap conductance relative to the GLRWOB transient. In fact,

Table 7-2

## Key Results of Sensitivity Studies for FWCF Transient

<u>Description of Modification to Base Model</u>	$\Delta Q$ (% NBR)	$\Delta q$ (% NBR)	$\Delta P_{VSD}$ (psi)	$\Delta RCPR$
<u>Nuclear Model</u>				
Void coefficient 13% more negative	+ 44.1	+ 2.1	- 0.8	+ 0.015
Scram reactivity reduced 10%	+ 8.8	+ 0.79	+ 1.6	+ 0.006
Prompt moderator heating reduced 25%	- 0.1	+ 0.58	+ 0.3	0.000
<u>Core Thermal-Hydraulic Modeling</u>				
Fuel rod gap conductance increased 25%	- 3.7	+ 0.33	- 0.5	- 0.004
Reduce initial core bypass flow by 20%	- 4.8	- 0.28	- 0.5	- 0.002
Eliminate core bypass flow junction 109	- 18.8	- 1.00	- 1.0	- 0.008
Remove all passive conductors	- 14.1	- 0.99	+ 1.2	- 0.006
Use HEM in thermal-hydraulic solution	- 40.1	- 1.93	+ 2.3	- 0.009
Reduce subcooled voids by 30%	+ 25.8	+ 1.15	- 0.2	+ 0.008
<u>Recirculation System Model</u>				
Jet pump M ratio increased 7%	+ 7.6	+ 0.54	+ 0.4	0.000
Jet pump head reduced 10%	- 1.0	- 0.06	- 0.1	+ 0.001
<u>Steam Line Modeling</u>				
Increase steam line inertia by 7%	+ 3.0	+ 0.16	- 0.1	- 0.001
Reduce steam line pressure drop by 10%	+ 11.3	+ 0.51	- 2.8	+ 0.005
Nominal relief valve opening delay	0.0	0.00	- 10.4	0.000
Increase rated turbine bypass capacity 10%	- 9.1	- 0.53	+ 0.1	- 0.003
Nominal bypass servo time constants	- 37.2	- 2.03	- 0.3	- 0.023
<u>Miscellaneous</u>				
Nominal RPT delay	- 6.9	- 0.44	- 0.5	- 0.001
Decrease maximum FW runout by 5% NBR	+ 3.7	- 0.28	- 0.1	- 0.001
Initialized for 100% NBR steam flow	- 19.1	- 5.58	- 5.8	+ 0.002
Nominal measured scram speed	- 45.7	- 2.65	- 6.4	- 0.014
Final feedwater enthalpy reduced 20 Btu/lb	+ 11.2	+ 3.38	+ 1.3	+ 0.004
Initiated on load line at reduced flow (approx. 71% rated)	- 86.5	- 28.7	- 26.7	- 0.004

- $\Delta Q$  = perturbed case peak power (% NBR) minus base case value  
 $\Delta q$  = perturbed case peak core average heat flux (% NBR) minus base case value  
 $\Delta P_{VSD}$  = perturbed case peak vessel dome pressure (psia) minus base case value  
 $\Delta RCPR$  = perturbed case CPR/ICPR minus base case value

lower sensitivities to all perturbations to core thermal-hydraulic models were exhibited for the FWCF event. In general, the direction of change in a result caused by a given model perturbation was the same for FWCF and GLRWOB; however, due to differences in timing of various phenomena, the reduction of core bypass flow by 20 percent and the use of the HEM thermal-hydraulic solution resulted in less severe values of RCPR for the FWCF while both caused more severe results for the GLRWOB transient. The major uncertainty component from core thermal-hydraulics model of the FWCF event (as for the GLRWOB) arose from the 30-percent reduction in subcooled voids.

#### 7.2.3 Recirculation System Model

The 7 percent increase in jet pump M ratio slightly increased the peak values of power, heat flux, and vessel pressure but by significantly smaller amounts than for the GLRWOB transient. The value of RCPR was not appreciably affected by the M ratio change. A 10-percent reduction in jet pump head caused very slightly less severe results for all key results except RCPR which increased by an insignificant amount (0.001).

#### 7.2.4 Steam Line Modeling

Increasing the steam line inertia by 7 percent had an insignificant effect on computed transient results for the FWCF. The importance of the timing of various phenomena is demonstrated by the fact that two key results were slightly more severe and two less severe for the FWCF but all four were more severe for the GLRWOB transient with increased steam line inertia.

The change in results caused by decreasing the steam line pressure drop was of comparable magnitude to that shown by the GLRWOB with RCPR

Increasing by 0.005. The use of a best-estimate relief valve opening delay reduced the maximum pressure by 10 psi but did not affect power, heat flux, or RCPR. This is in contrast to the nominal relief valve modeling results for the GLRWOB transient where the timing of the valve opening was such that RCPR was influenced for a short time.

Additional sensitivity studies were performed for the FWCF event to assess sensitivity to turbine bypass modeling. A 10-percent increase (2.62-percent NBR steam flow) in rated turbine bypass flow capability produced a modest decrease in all key results. The use of nominal turbine bypass servo delays and time constants greatly reduced the value of RCPR relative to the base case using licensing basis (upper limit) time constants.

#### 7.2.5 Miscellaneous

Only minor changes in key results occurred for the FWCF event when a nominal recirculation pump trip delay was utilized or when the maximum runout capability of the feedwater pumps was decreased by 5-percent NBR to the nominal value.

The use of nominal measured scram speeds results in a large decrease in severity of the FWCF event as expected. The reduction in final feedwater enthalpy produces a slightly more severe transient than the licensing basis result initiated from maximum feedwater enthalpy because the same increase in feedwater flow following the controller failure results in a greater increase in core inlet subcooling. The initiation of the FWCF event from reduced power may also result in a slightly more severe transient since the amount of increase in feedwater flow to maximum runout is larger. The larger reduction in core inlet subcooling for a greater

feedwater flow increase may be sufficient to overcome the less severe pressurization rate from reduced power yielding a slightly larger value of RCPR. For the base case used in these studies (Browns Ferry unit 3 EOC5); however, this effect was not sufficient to yield a net increase in RCPR. For core flows less than 75 percent of rated the operating limit CPR is always increased by multiplying by the  $K_f$  factor in the unit technical specifications. The  $K_f$  multiplier is computed to provide protection for a slow pump runout transient and the increase in operating limit CPR required by the  $K_f$  multiplier is significantly larger than the FWCF event would necessitate.

To account for any potential nonconservatism in the licensing basis FWCF analysis from 105-percent steam flow and maximum feedwater enthalpy, a 0.03 adder is applied to the RETRAN results for the FWCF event as indicated in table 6-4. The 0.03 adder is larger than any potential nonconservatism arising from reduced feedwater enthalpy or reduced power operations not covered by the  $K_f$  multiplier.

### 7.3 MSIVC Sensitivity Studies

Since main steam isolation valve closure with indirect scram on high power is not a transient expected to occur during the life of a plant it is not analyzed for meeting the safety-limit CPR and no RCPR sensitivity results will be presented. The primary purpose of the MSIVC event is to demonstrate compliance with the 1375 psig limit on maximum vessel pressure, therefore the primary sensitivity result is the change in peak vessel lower plenum pressure.

A summary of a representative sample of the sensitivity studies performed for the MSIVC event is shown in table 7-3. The manner in which

Table 7-

## Key Results of Sensitivity Studies for MSIVC (Flux Scram) Event

<u>Description of Modification to Base Model</u>	<u><math>\Delta Q</math></u> <u>(% NBR)</u>	<u><math>\Delta q</math></u> <u>(% NBR)</u>	<u><math>\Delta P_{VLP}</math></u> <u>(psi)</u>
<u>Nuclear Model</u>			
Void coefficient 13% more negative	+ 22.0	+ 1.05	+ 2.4
Scram reactivity reduced 10%	+ 17.7	+ 1.14	+ 3.4
Doppler coefficient reduced 10%	+ 13.6	+ 0.75	+ 1.3
Prompt moderator heating reduced 25%	+ 31.7	+ 2.64	+ 1.9
<u>Core Thermal-Hydraulics Modeling</u>			
Fuel rod gap conductance increased 25%	- 48.7	+ 0.18	- 2.0
Reduce initial core bypass flow by 20%	+ 5.4	+ 0.59	+ 0.6
Eliminate core bypass flow junction 109	- 14.1	- 0.57	- 0.6
Remove all passive conductors	- 45.7	- 2.43	+ 2.0
Use HEM in thermal-hydraulic solution	+ 55.2	+ 4.85	+ 10.3
Reduce subcooled voids by 30%	+ 35.6	+ 1.24	+ 1.5
<u>Recirculation System Model</u>			
Double recirc loop fluid inertia	- 2.2	- 0.06	+ 0.2
Jet pump M ratio increased 7%	+ 29.2	+ 1.56	+ 2.0
Increased M-G inertias by 25%	+ 0.1	+ 0.01	+ 0.2
<u>Steam Line Model</u>			
Reduce steam line volume 5%	+ 5.6	+ 0.21	+ 0.1
Increase steam line inertia by 7%	- 4.3	+ 0.04	- 0.6
Nominal relief valve capacity	0.0	0.00	- 10.8
<u>Miscellaneous</u>			
Reduce FW flow pressure correction by 33%	+ 1.4	+ 0.12	+ 2.0
Initialized for 100%-NBR steam flow	- 45.8	- 7.53	- 14.5
Nominal measure scram speed	- 64.8	- 4.31	- 13.7

$\Delta Q$  = perturbed case peak power (% NBR) minus base case value

$\Delta q$  = perturbed case peak core average heat flux (% NBR) minus base case value

$\Delta P_{VLP}$  = perturbed case peak vessel lower plenum pressure (psia) minus base case value

the model perturbations were introduced is the same as was described for the GLRWOB transient. The major effects on peak pressure were found to be due to the scram reactivity and slip (HEM) uncertainties. However, the combined uncertainty of the nonconservative components was only 12 psi which is of comparable magnitude to the conservatism in the relief valve capacity used in the licensing basis modeling and less than the conservatism due to the use of upper limit technical specification scram speeds. An additional large conservatism (not quantified in this study) is due to the assumed MSIV closure characteristics which was very nonlinear allowing the flow area to be reduced by 99 percent after 1.7 seconds and the valves to be fully closed in the minimum technical specification time of 3 seconds.

References

- 7-1. S. L. Forkner, G. H. Meriwether, and T. D. Beu, "Three-Dimensional LWR Core Simulation Methods," TVA-TR78-03A, 1978.
- 7-2. TVA-TR79-01A, "Verification of TVA Steady-State BWR Physics Methods," January 1979.
- 7-3. A. Premoli, et al., "An Empirical Correlation for Evaluating Two-Phase Mixture Density Under Adiabatic Conditions," An Informal Contribution to the Private Meeting, Heat Transfer Laboratory, Grenoble, France, 1970.
- 7-4. B. L. Darnell, T. D. Beu, and G. W. Perry, "Methods for the Lattice Physics Analysis of LWRs," TVA-TR78-02A, 1978.
- 7-5. L. M. Petrie and N. F. Cross, "KENO IV - An Improved Monte Carlo Criticality Program," ORNL-4938, 1975.
- 7-6. E. Hellstrand, "Measurements of the Effective Resonance Integral in Uranium Metal and Oxide in Different Geometries," J. Appl. Phys., 28, 1493-1509 (1957).
- 7-7. E. Hellstrand, P. Blomberg, and S. Horner, "The Temperature Coefficient of the Resonance Integral for Uranium Metal and Oxide," Nucl. Sci. Eng., 8, 497 (1960).
- 7-8. "Qualification of the One-Dimensional Core Transient Model for Boiling Water Reactors," NEDO-24154, Volume 1, pages Q5-1 to Q5-3, October 1978.
- 7-9. G. S. Lellouche and B. A. Zolotar, "A Mechanistic Model for Predicting Two-Phase Void for Water in Vertical Tubes, Channels, and Rod Bundles," EPRI (to be published).
- 7-10. B. A. Zolotar, "An Approximate Form of the EPRI-Void Formulation Model," EPRI (to be published).

## 8. ALLOWANCES FOR MODEL UNCERTAINTIES

The procedure to be employed by TVA in determining updates to unit technical specifications relating to the operating limit CPR for pressurization transients will be consistent with the approach utilized in current technical specifications for the Browns Ferry units. The "deterministic" value of  $\Delta\text{CPR}$  (or  $\text{RCPR}$ ) from the RETRAN model for the GLRWOB and FWCF events with licensing basis inputs (as described in chapter 6) will be corrected to values which yield 95-percent probability with 95-percent confidence (95/95) that the safety-limit CPR (1.07) will not be violated by the event if initiated at or above the operating limit CPR determined by adding the adjusted  $\Delta\text{CPR}$  to the safety limit. Two separate methods are utilized for determining the adjustment to the deterministic  $\Delta\text{CPR}$ s. These methods (referred to as "option A" and "option B") will be described in the sections to follow and the manner in which they will be employed in updating the unit technical specifications described.

### 8.1 Option A Operating Limit MCPR

The option A approach takes no credit for the large conservatisms in the licensing basis models and inputs which were demonstrated in chapter 7. The uncertainty in transient  $\text{RCPR}$  as computed by the model is determined based on the sensitivity studies. The sensitivity study components in table 7-1 indicated by an asterisk (\*) in the last column are considered applicable in setting the model uncertainty. Table 8-1 shows the combined uncertainty for each major model component (in terms of  $\text{RCPR}$ ) and the overall model uncertainty. Since upper limit component and equipment

uncertainties were utilized in the sensitivity studies it is reasonable to equate the 0.041 RCPR uncertainty as being an upper bound or 95/95 level. The approach utilized in applying the option A uncertainty is shown by equation 8-1.

$$\text{Option A OLMCPR} = 1.041 * (\text{SLCPR} + \Delta\text{CPR}) \quad (8-1)$$

Where SLCPR is the safety-limit CPR value of 1.07 and  $\Delta\text{CPR}$  is the deterministic value calculated by the RETRAN model for either the FWCF or GLRWOB transient. Application of equation 8-1 to the RETRAN model deterministic  $\Delta\text{CPR}$  values from table 6-4 results in operating limit MCPR values of 1.34 and 1.29 for the GLRWOB and FWCF events, respectively.

Table 8-1

Components in Browns Ferry RETRAN Model Uncertainty

<u>Component</u>	<u>Uncertainty in RCPR</u>
Nuclear Model	0.033
Core Thermal-Hydraulics Modeling	0.016
Recirculation System Model	0.013
Vessel and Steam Line Nodes	<u>0.013</u>
Combined uncertainty	0.041

## 8.2 Option B Operating Limit MCPB

The option A operating limit MCPB is very conservative in that no credit is taken for conservatisms inherent in the licensing basis analyses including the significant conservatisms in the use of technical specification upper limits on average control rod motion following scram and the use of 105-percent NBR initial steam flow. The conservatisms are compounded by the use of a model uncertainty penalty to the operating limit CPR. The option B method is an approach to reduce the unwarranted conservatism introduced by compounding the uncertainties. The option B approach utilizes the conservatism inherent in the statistical variation of expected operating conditions (for initial steam flow and scram speed) from the limiting conditions assumed in licensing basis calculations to compensate for potential nonconservatisms resulting from uncertainty in model predictions. Statistical convolution of initial steam flow and scram speed uncertainties with the model uncertainty was employed to determine statistical adjustment factors (SAFs) to the deterministic licensing basis RCPR value which maintain a 95-percent probability (at 95-percent confidence level) that the safety-limit CPR will not be violated for the limiting pressurization transients. The statistical adjustment factor determination will be based on the Browns Ferry unit 3 projected cycle 5 conditions but this cycle is representative of expected operation for all three Browns Ferry units and the SAFs are generically applicable to future operating cycles at all three Browns Ferry units.

### 8.2.1 Statistical Process for Margin Evaluation

The objective of the statistical evaluation is development of the probability distribution for RCPR given the statistical distribution of the

key transient input variables. The probability distribution of RCPR is then utilized to obtain the value of RCPR which has 95-percent probability at 95-percent confidence of not being exceeded by the operating plant if the limiting pressurization event occurs. The direct approach to developing the RCPR probability distribution would be to run trials with the RETRAN model with the key inputs selected randomly from their uncertainty distribution. However, the Monte Carlo approach requires a large number of trials to develop a precise probability distribution so direct simulation of each trial with the RETRAN model is impractical. Instead a response surface is constructed which predicts the RETRAN model calculated value of RCPR as a function of the value of the key inputs. The response surface is developed by fitting model results to a polynomial with the key transient inputs as independent variables. The advantage of the response surface is that far fewer model calculations are required to develop an accurate response surface than to directly develop the probability distribution on RCPR.

#### 8.2.2. Model Response Surfaces

The response surfaces used in the analyses to be presented have the form shown in equation 8-2.

$$RCPR = (A_0 + A_1 * SF + A_2 * SF^2 + A_3 * SS + A_4 * SF * SS + A_5 * SS^2 + URS) * URM \quad (8-2)$$

where,

SF = random value of initial steam flow (% NBR) minus the nominal value

SS = random value of time (seconds) to 20% scram insertion minus the nominal value

URS = random response surface fitting error

URM = random fractional uncertainty in RETRAN model predictions

and the  $A_i$  are fitting coefficients unique to each response surface.

In order to develop the fitting coefficients ( $A_i$ ) for the response surfaces 17 RETRAN simulations were performed for each one. The procedure used was an augmented variation of the factorial design process for three parameter levels (reference 8-1). Five values of each of the key input variables (steam flow and scram speed) over the approximate range of  $\pm 4.5$  standard deviations were utilized. A matrix of possible combinations of key inputs for model calculations with these values is shown in table 8-2 with combinations actually used denoted by an "X." The value of the input variable index is used to denote the relative deviation of the variable value from its expected or mean value.

The 17 cases defined by table 8-2 were run for the GLRWOB and FWCF events at end of cycle (all control rods withdrawn) and for an earlier point in the cycle for which some control rods were still initially present in the core. Tables 8-3 and 8-4 show the comparison of fitted response surface RCPR values to the RETRAN model calculation for the GLRWOB and FWCF events, respectively. A standard least squares fitting technique was used and the low order (six constant) equation resulted in very small fitting errors. The 95-percent confidence level (upper bound) estimate of the standard deviation of the fitting errors was determined by use of chi-squared statistics. The reliability of the response surface was also tested by developing the fitting constants utilizing only a portion of the data and then comparing to the error obtaining using all 17 points. The fitting coefficients were not significantly affected and the standard deviation of the fitting error was of a similar size as obtained when all data points were used in the fit. The 95-percent confidence standard deviation (with a zero mean) for the fitting error was employed to generate

Table 8-2

## Matrix of Response Surface Runs

		Initial Steam Flow Index				
		-2	-1	0	+1	+2
Initial Scram Speed Index	-2	X		X		X
	-1		X	X	X	
	0	X	X	X	X	X
	+1		X	X	X	
	+2	X		X		X

X indicates RETRAN model calculations performed

Table 8-3

## Accuracy of Response Surface for GLRWOB at End of Cycle

<u>Observation No.</u>	<u>Model RCPR</u>	<u>Fit RCPR</u>	<u>Difference</u>
1	0.11350	0.11397	-0.00047
2	0.12510	0.12485	0.00025
3	0.11750	0.11974	-0.00224
4	0.10830	0.10755	0.00075
5	0.09790	0.10048	-0.00258
6	0.16990	0.17192	-0.00202
7	0.14500	0.14288	0.00212
8	0.08340	0.08525	-0.00185
9	0.05590	0.05666	-0.00076
10	0.18450	0.18640	-0.00190
11	0.06430	0.06395	0.00035
12	0.15490	0.15483	0.00007
13	0.04960	0.04678	0.00282
14	0.15410	0.14954	0.00456
15	0.09140	0.09012	0.00128
16	0.13800	0.13556	0.00244
17	0.07690	0.07973	-0.00283

Average Difference = 0.00000  
 Standard Deviation = 0.00214  
 95% Confidence S.D. = 0.00303

Table 8-4

## Accuracy of Response Surface for FWCF at End of Cycle

<u>Observation No.</u>	<u>Model RCPR</u>	<u>Fit RCPR</u>	<u>Difference</u>
1	0.09510	0.09549	-0.00039
2	0.08810	0.08929	-0.00119
3	0.09530	0.09293	0.00237
4	0.09530	0.09697	-0.00167
5	0.09770	0.09737	0.00033
6	0.10940	0.10934	0.00006
7	0.10350	0.10373	-0.00023
8	0.08420	0.08465	-0.00045
9	0.07060	0.07117	-0.00057
10	0.10460	0.10538	-0.00078
11	0.06140	0.06273	-0.00133
12	0.11050	0.10898	0.00152
13	0.07620	0.07528	0.00092
14	0.10320	0.10173	0.00147
15	0.08480	0.08153	0.00327
16	0.10200	0.10465	-0.00265
17	0.08600	0.08668	-0.00068

Average Difference = 0.00000  
Standard Deviation = 0.00151  
95% Confidence S.D. = 0.00214

the values of the response surface uncertainty (variable URS in equation 8-2) by selecting randomly from a normal distribution for each trial evaluation of the response surface. Application of the W-test (reference 8-2) to the fitting errors showed no basis to reject the assumption of normality.

The trial values of initial steam flow (variable SF in equation 8-2) and time to 20-percent scram insertion (variable SS) were also assumed to be normally distributed. The mean initial steam flow was 100-percent NBR with a 2-percent NBR standard deviation (reference 8-3). The mean time to 20-percent control rod insertion following scram solenoid deenergization was assumed to be 0.71 seconds with a standard deviation of 0.053 seconds. These values are conservative relative to measured data for Browns Ferry and consistent with option B scram time conformance testing in current Browns Ferry Technical Specifications (reference 8-4).

Two measures of the uncertainty associated with predictions of transient RCPR with the Browns Ferry RETRAN model are available. Neglecting any conservative biases the sensitivity studies in chapter 7 were employed to arrive at an estimated uncertainty in RCPR of 0.041 in section 8.1. Since the base value of RCPR for the GLRWOB transient is 0.17 the estimated model uncertainty (2 standard deviations) is 24 percent. A second measure of the model uncertainty was obtained by comparing the differences in RCPR between the normalized model calculations and those inferred from measured data for the Peach Bottom turbine trip test presented in table 4-12. Based on this comparison the model predictions conservatively overestimated RCPR by an average of 6.6 percent with a standard deviation of 2.6 percent. Using the chi-squared test these three data points yield a 95-percent confidence model uncertainty (2 ) of 23 percent, neglecting the conservative bias.

Based on the comparisons to Peach Bottom turbine trip test data and the sensitivity study results, the model uncertainty (URM variable in equation 8-2) was conservatively assumed to be normally distributed with a mean of 1.0 and standard deviation of 0.125 (model uncertainty of 25 percent).

### 8.2.3 Statistical Adjustment Factors

The fitted response surface equation (8-2) along with the uncertainty distribution for each of the four input variables was evaluated for several hundred thousand trials. Each trial selects a random value for each of the four variables in accordance with their assumed uncertainty distribution, and equation 8-2 is evaluated to obtain the corresponding RCPR value. The maximum range of RCPR values was divided into approximately 100,000 intervals to obtain a resolution of RCPR better than  $10^{-4}$ . A count was kept of the number of trials which resulted in an RCPR value in each interval, thus generating a probability density function (PDF) for RCPR.

To obtain the RCPR value which is greater than 95 percent of the trials the PDF is integrated from the lowest interval up to the value at which 95 percent of the trials have been accumulated. In general to obtain the RCPR value for a prescribed probability (P) and one-sided confidence interval (C) after N trials have been performed, the number of trials which must be accumulated (n) by the integration is:

$$n = PN + g(C) * [NP(1-P)]^{1/2} \quad (8-3)$$

where  $g(C)$  is 1.645 for  $C$  equal to 95 percent. Equation 8-3 is based on the normal distribution approximation of a binominal distribution (reference 8-5) and has been shown to be very accurate for large values of  $N$  and  $C$ .

After integrating the PDF up to a value of RCPR such that  $n$  trials have been accumulated, RCPR (95/95), the licensing basis value of RCPR is subtracted from RCPR (95/95) to obtain the statistical adjustment factor. Table 8-5 shows the resulting SAFs for the GLRWOB and FWCF events of EOC and for a point with initial control rod insertion (MOC).

Table 8-5

## Values of Statistical Adjustment Factors for Browns Ferry RETRAN Model

	<u>SAF</u>
GLRWOB at EOC	- 0.025
GLRWOB at MOC	- 0.022
FWCF at EOC	+ 0.007
FWCF at MOC	- 0.002

The SAFs are used to adjust the deterministic licensing basis RCPR values by equation 8-4.

$$\text{Option B OLMCPR} = \frac{\text{SLCPR}}{1 - [\text{RCPR} + \text{SAF}]} \quad (8-4)$$

The resulting option B operating limit MCPR value based on the deterministic values from table 6-4 is 1.25 for both the GLRWOB and FWCF events at end of cycle 5 for Browns Ferry unit 3.

### 8.3 Determination of Actual Operating Limit MCPR

The overall operating limit for MCPR specified as a limiting condition for operation in a unit's technical specifications is specified as a function of scram time (with adjustments based on core flow) based on the envelope of maximum OLMCPR values resulting from all safety analyses. Since the primary difference between the option A and B OLMCPRs is due to the assumed scram speeds, the applicable limit is determined by interpolation between these limits based on the actual average scram speed measured during the operating cycle.

The Browns Ferry technical specifications have surveillance requirements that all control rods be scram tested after each refueling outage and 10 percent of the control rods at 16-week intervals. The surveillance testing data is utilized to compute the average scram time to 20-percent insertion from the fully withdraw position ( $\tau_{avg}$ ):

$$\tau_{avg} = \frac{\sum_{i=1}^n \tau_i}{n} \quad (8-5)$$

where  $\tau_i$  is the 20-percent insertion time of rod  $i$  and  $n$  is the total number of surveillance rod tests performed to date in the cycle including the  $N$  active rods measured at beginning of cycle.

The interpolation between option A and B OLMCPRs is based on the fractional difference ( $\tau$ ) of the average measured scram time ( $\tau_{avg}$ ) between the option A scram time ( $\tau_A = 0.90$  seconds to 20-percent insertion which is the upper conformance limit on average scram time) and the option B adjusted scram time.

$$\tau = \text{maximum of } 0 \text{ and } \frac{\tau_{\text{avg}} - \tau_B}{\tau_A - \tau_B} \quad (8-6)$$

with:

$$\tau_B = \mu + 1.65 \left[ \frac{N}{n} \right]^{1/2} \sigma \quad (8-6)$$

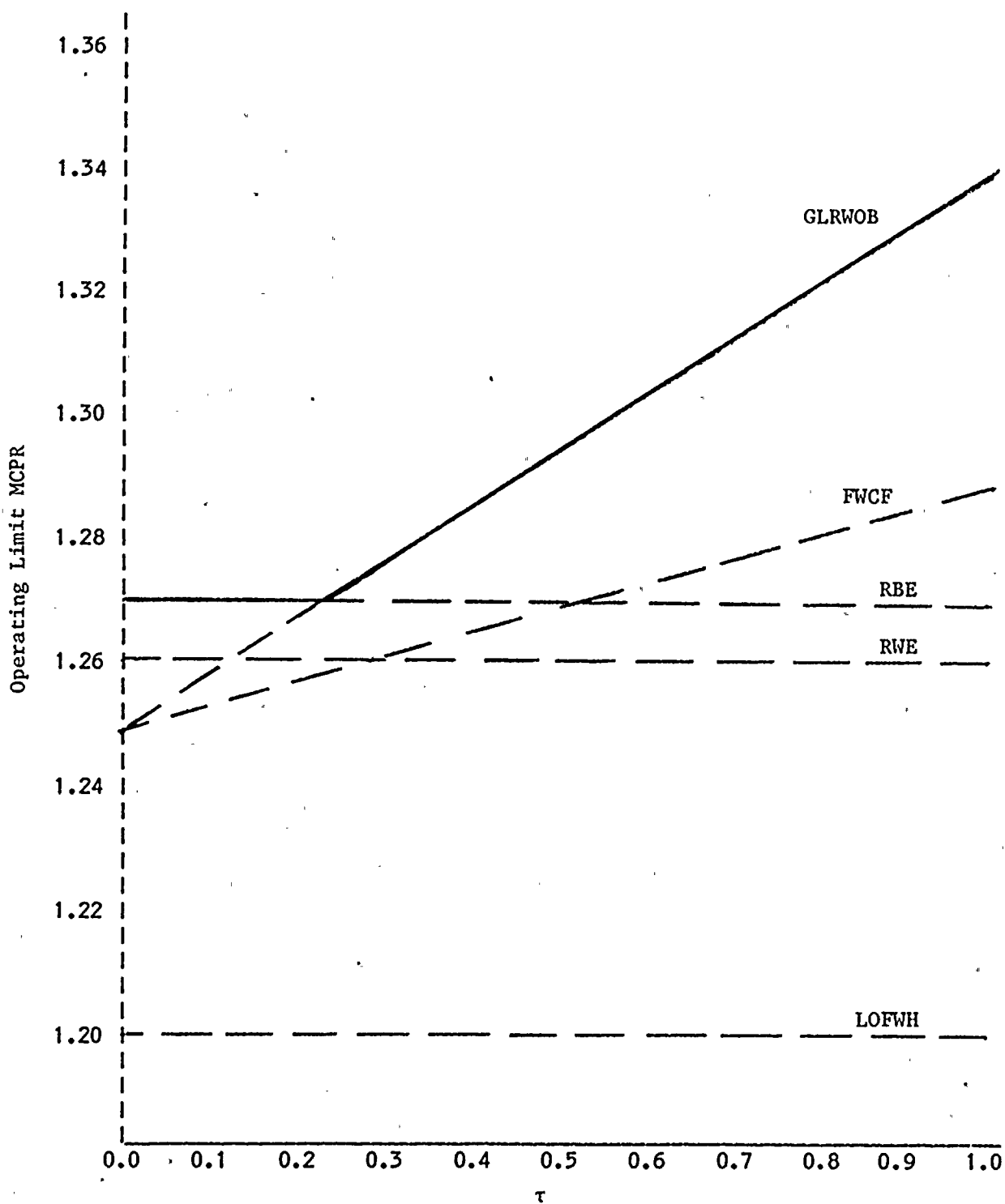
where  $\mu$  is the average time to 20-percent scram insertion (0.71 seconds) utilized in the option B analyses and  $\sigma$  is the corresponding scram time standard deviation (0.053 seconds).

The OLMCPR required by the GLRWOB and FWCF events by TVA analyses is shown in figure 8-1 as a function of  $\tau$ . Also shown on figure 8-1 are the OLMCPR values required by the nonpressurization transient safety analyses, in particular, the 100°F loss of feedwater heating (LOFWH) event, the control rod withdrawal error (RWE) at high power, and the rotated bundle error (RBE) analyses.

The overall operating limit MCPR (before correction for core flow) is obtained as an upper envelope of all safety analysis results and is indicated by the solid line in figure 8-1.

Figure 8-1

Hypothetical Browns Ferry Unit 3, Cycle 5, Operating Limit MCPR  
for GE P8 x 8R Fuel Bundles Based on TVA Methods



REFERENCES

- 8-1 Probability and Statistics for Engineers. Irwin Miller and John E. Freund, Prentiss-Hall, Inc., 1977, pages 375-418.
- 8-2 Statistical Models in Engineering. Gerald J. Hahn and Samuel S. Shapiro, John Wiley & Sons, Inc., 1967, pages 294-302.
- 8-3 NRC Safety Evaluation for the General Electric Topical Report, Qualification of the One-Dimensional Core Transient Model for Boiling Water Reactors, NEDO-24154 and NEDE-24154-P, Volumes I, II, and III, June 1980.
- 8-4 "Browns Ferry Nuclear Plant Unit 3 Technical Specifications," Tennessee Valley Authority.
- 8-5 Statistical Models in Engineering. Gerald J. Hahn and Samuel S. Shapiro, John Wiley & Sons, Inc., 1967, pages 144-171.